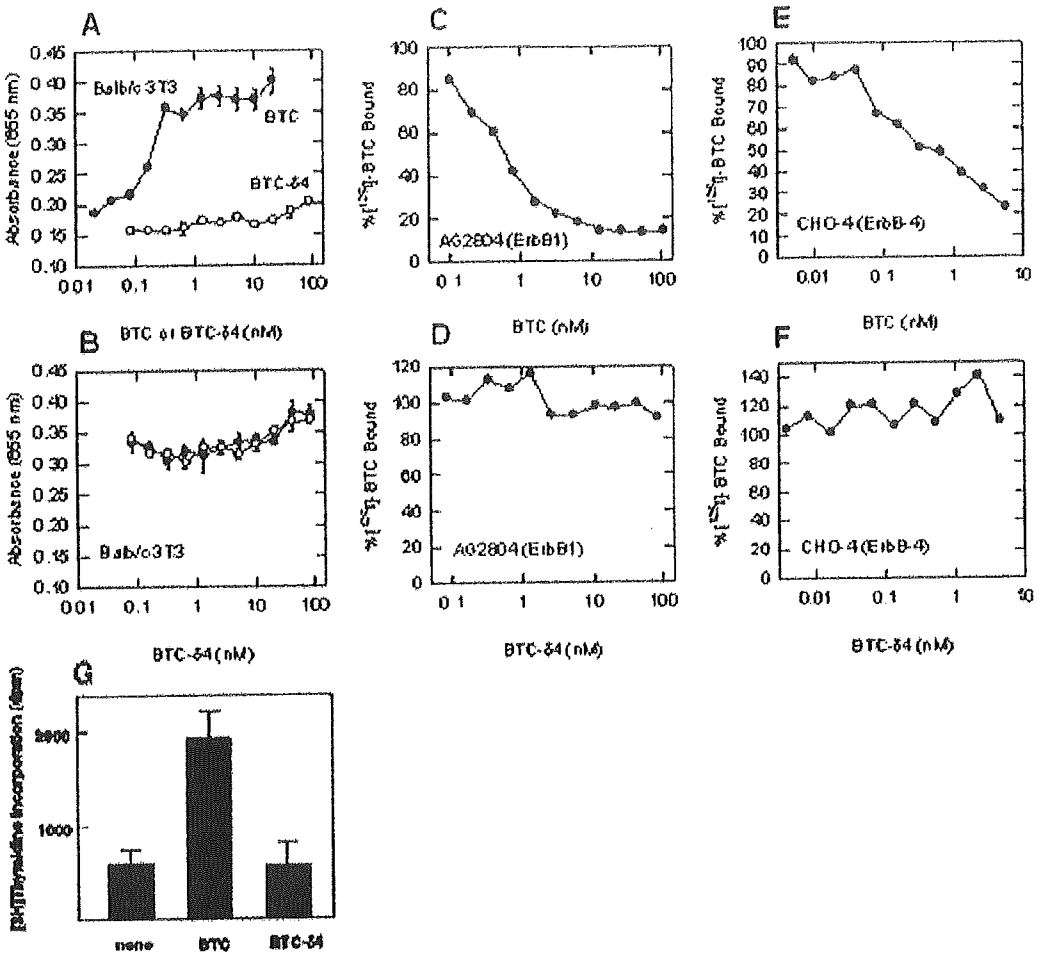

FIG. 4. BTC, but not BTC-δ4, stimulates the proliferation of Balb/c 3T3 and INS-1 cells. Balb/c 3T3 fibroblasts were incubated with increasing concentrations of either BTC or BTC-δ4 alone (A) or increasing concentrations of BTC-δ4 in the presence of a fixed concentration of BTC (1 nM) (B). Competitive binding of [^{125}I]-labeled BTC, in the presence of increasing concentrations of BTC or BTC-δ4, to either AG2804 cells expressing ErbB1 (C and D) or CHO cells transfected with ErbB4 (E and F). G, INS-1 cells were incubated for 48 h with 1 nM BTC or 1 nM BTC-δ4, and [^{3}H]thymidine incorporation was measured. Values are the mean ± SE of four experiments.

in the cell lysate (~20 kDa) and on the cell surface (Fig. 2, A and B).

Recombinant production of BTC-δ4

To characterize the biological activity of BTC-δ4, we cloned the cDNA (Asp_{32}-Ala_{129}; without the signal peptide) into the pET-32a expression vector and expressed the protein as a thioredoxin fusion in *Escherichia coli* BL21*trxB* (DE3) (Fig. 3A). This strain is deficient in thioredoxin reductase, allowing for disulfide bond formation in the cytoplasm. The purified thioredoxin fusion protein was cleaved with enterokinase to release BTC-δ4, which was purified to homogeneity by RP-HPLC (Fig. 3B). As a control, we also generated BTC (Asp_{32}-Tyr_{111}) with this system and purified it in the same manner. The purity of both the BTC and BTC-δ4 preparations was further confirmed by N-terminal sequence analysis (five cycles), which gave the expected N-terminal sequence with an approximate purity of more than 95% (data not shown). The molecular mass of recombinant BTC and BTC-δ4 determined by electrospray ionization mass spectrometry was 9,211.35 ± 0.29 Da and 11,450.26 ± 0.23 Da, respectively, which is consistent with the calculated theoretical masses of 9,249 and 11,452 Da (data not shown). After SDS-PAGE and silver staining, a single band at approximately 9 kDa and 11.5 kDa was obtained for BTC and BTC-δ4 detected under reducing or nonreducing conditions (data not shown).

BTC-δ4 does not bind or activate either ErbB1 or ErbB4

BTC stimulated the proliferation of Balb/c 3T3 fibroblasts in a dose-dependent fashion (Fig. 4A). In contrast, BTC-δ4 did not stimulate cell proliferation, even at concentrations as high as 100 nmol/liter (Fig. 4A), or antagonize the effects of BTC in this cell line (Fig. 4B). Consistent with these results, BTC, but not BTC-δ4, could displace [^{125}I]-BTC from ErbB1 receptors present on human lung fibroblasts (AG2804) (Fig. 4, C and D) and induce ErbB1 receptor autophosphorylation (Fig. 5). Similarly, BTC, but not BTC-δ4, competed for ErbB4 receptor binding (Fig. 4, E and F) and induced ErbB4 receptor tyrosine phosphorylation (Fig. 5). These results indicate that, unlike BTC, BTC-δ4 displays no affinity toward either ErbB1 or ErbB4. We also examined the effect of BTC and BTC-δ4 on DNA synthesis in INS-1 cells. As shown in Fig. 4G, BTC

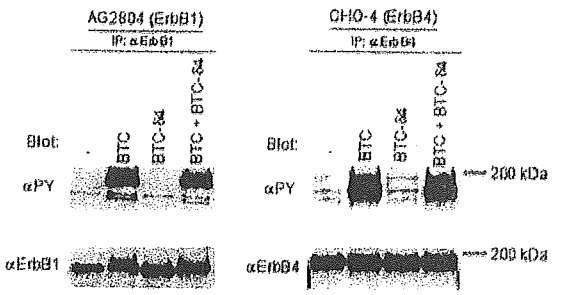

FIG. 5. BTC, but not BTC-δ4, induces ErbB1 and ErbB4 receptor tyrosine phosphorylation in AG2804 and CHO-ErbB4 cells, respectively. Lysates from untreated (–) or treated (10 nmol/liter BTC, 10 nmol/liter BTC-δ4, or 10 nmol/liter BTC + 10 nmol/liter BTC-δ4) cells were immunoprecipitated (IP) with either anti-ErbB1 (AG2804) or anti-ErbB4 (CHO-ErbB4) antibodies and then blotted and probed with antiphosphotyrosine antibody (αPY). Blots were also stripped and reprobed with anti-ErbB1 or anti-ErbB4 antibodies.

stimulated DNA synthesis in INS-1 cells, whereas BTC-δ4 did not.

BTC-δ4 induces the differentiation of pancreatic β-cells

BTC is known to stimulate the differentiation of pancreatic β-cells (9–14), and there is some evidence to suggest that this may occur through a unique non-ErbB cell surface receptor (22). To examine the effect of BTC-δ4 on the differentiation of pancreatic β-cells, we used the model cell line AR42J-B20; a subclone of AR42J, an amylase-secreting pancreatic tumor cell line. In these cells, BTC acts coordinately with activin A and converts them to insulin-secreting cells (9). Activin A also induces apoptosis in these cells and, in the absence of a survival factor, many of the activin-treated cells die by apoptosis after the conversion to pancreatic polypeptide (PP)-producing cells (23). BTC exerts two effects in AR42J-B20 cells: BTC inhibits apoptosis induced by activin A; and, second, converts them to insulin-producing cells (9, 23). As shown in Fig. 6A, AR42J-B20 cells differentiated into insulin-producing cells by a combination of activin A and BTC. Quantitatively, 78 ± 6.5% of the cells (mean ± SE; n = 4) became insulin-positive after 48 h. Cells treated with activin A and BTC exhibited extended processes and expressed immunoreactive insulin (Fig. 6C). Cells treated with a combination of activin A and BTC-δ4 also became insulin-positive; 72 ± 4.5% (n = 4) of the cells became insulin-positive after 48 h (Fig. 6B). It should be noted that cells treated with activin A and BTC-δ4 were also positive for C-peptide (Fig. 6G). In contrast to cells treated with activin A and BTC, the morphology of cells treated with activin A and BTC-δ4 was quite different. Some of the insulin-positive cells displayed extended processes, but most of them remained circular in appearance. The nuclei of these cells were condensed and, in some instances, were either fragmented or absent (Fig. 6, B and D), characteristic of cell death by apoptosis. Consistent with this notion, many of the cells treated with activin A and BTC-δ4 were TUNEL-positive (Fig. 6F), compared with only a small fraction of cells treated with activin A and BTC (Fig. 6E). To further confirm the effect of BTC-δ4 on the survival of AR42J-B20 cells, we measured the changes in the number of viable cells after treatment with activin A and either BTC or BTC-δ4. After 48 h, the number of viable cells treated with activin A and BTC was 78.8 ± 4.2% of the number of cells seeded. In contrast, the number of viable cells treated with activin A and BTC-δ4 was significantly lower (21.8 ± 3.2%) ($P < 0.005$). Taken together, BTC-δ4 was as effective as BTC in stimulating the differentiation of AR42J-B20 cells; however, BTC-δ4 was much less potent in promoting survival of these cells. Note that BTC-δ4 alone did not induce differentiation of AR42J-B20 cells. Also, BTC-δ4 did not affect survival of these cells. When both BTC and BTC-δ4 were administered together with activin A, there was a small additivity in the actions of BTC and BTC-δ4, and 88 ± 4.5% of the cells became insulin-positive.

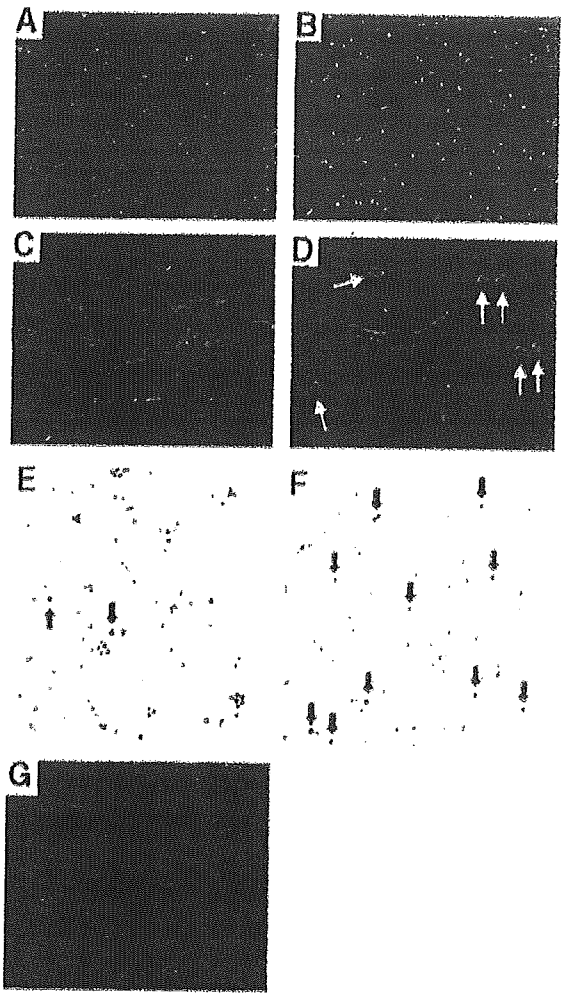

FIG. 6. The effects of BTC and BTC-δ4 on the differentiation and apoptosis of AR42J cells. AR42J-B20 cells were incubated for 48 h with 2 nmol/liter activin A and either 1 nmol/liter BTC (A and C) or BTC-δ4 (B and D), fixed, and then stained with antiinsulin antibody (*red*) and DAPI (*blue*) to stain nuclei. In cells treated with activin A and BTC-δ4, many cells expressed insulin, but nuclei were fragmented (*arrow*) or lost. Cells were also incubated with activin A and BTC-δ4 and stained with anti-C-peptide antibody (*red*) (G). Magnification, A and B, ×100; C, D, and G, ×400. E and F, AR42J-B20 cells were treated with 2 nmol/liter activin A and either 1 nmol/liter BTC (E) or BTC-δ4 (F) for 48 h, and the degree of apoptosis was detected by TUNEL. TUNEL-positive cells are indicated (*arrow*).

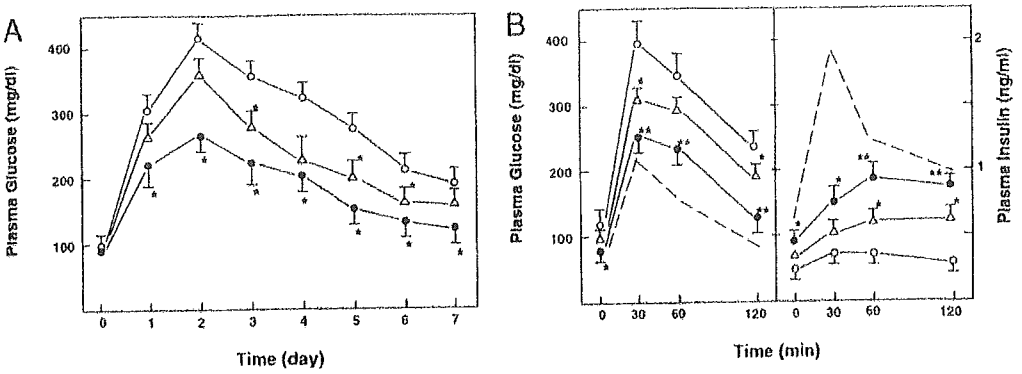

FIG. 7. BTC-δ4 administration to STZ-treated rats reduces the plasma glucose concentration and improves glucose tolerance. A, STZ (85 μg/g) was injected on d 0 (neonate of 1 d old), and daily injection of BTC or BTC-δ4 (1 mmol/liter) was started from d 0, for 5 d, and the plasma glucose concentration was measured. Values are the means ± SE; STZ group (n = 5); STZ/BTC-δ4 group (n = 5); STZ/BTC group (n = 5); *, $P < 0.05$ *vs.* the STZ group. B, Glucose tolerance test was performed on 2-month-old rats as described *Materials and Methods*. *Left panel*, Changes in the plasma glucose concentration. *Right panel*, Changes in the plasma insulin concentration. Values are the means ± SE; STZ group (n = 5); STZ/BTC-δ4 group (n = 5); STZ/BTC group (n = 5); (---), normal SD rats (n = 3); *, $P < 0.05$ *vs.* STZ group; **, $P < 0.01$ *vs.* STZ group.

BTC-δ4 administration to STZ-treated rats reduces the plasma glucose concentration and improves glucose tolerance

To investigate further the β-cell differentiating activity of BTC-δ4, we administered BTC-δ4 to neonatal STZ-treated rats. In STZ-treated neonatal rats, the plasma glucose concentration increased markedly and peaked on d 2 (>400 mg/dl) (Fig. 7A), thereafter declining gradually although still significantly higher compared with control rats after 2 months (Table 1). In STZ-treated rats administered BTC-δ4, the plasma glucose concentration was significantly lower on d 1, and the peak value was markedly reduced (Fig. 7A). The plasma glucose concentration was also reduced thereafter, until 2 months (Table 1). In contrast, BTC was less potent in improving hyperglycemia (Fig. 8A and Table 1). We also administered BTC and BTC-δ4 simultaneously, but the effect was not different from that obtained by BTC-δ4 alone (data not shown). At 2 months of age, ip glucose tolerance tests were performed. In STZ-treated rats, the glucose response to ip glucose-loading was markedly impaired; whereas in STZ-treated rats administered BTC-δ4, the glucose response was significantly improved (Fig. 7B). BTC-δ4 also increased the insulin response; but, compared with normal rats, the insulin response to ip glucose-loading was still delayed. In BTC-treated rats, glucose tolerance was improved, but the effect of BTC was less than that of BTC-δ4 (Fig. 7B). Moreover, the insulin content and the β-cell mass were significantly increased in BTC-δ4-treated rats (Table 1), and histological analysis of pancreatic tissue on d 4 indicated that BTC-δ4 significantly increased the numbers of PDX-1-positive ductal cells and ICCs (Fig. 8). We also examined the effect of BTC and BTC-δ4 on replication of insulin-positive cells. On d 4, the numbers of bromodeoxyuridine/insulin double-positive cells in saline-, BTC-, and BTC-δ4-treated rats were 5.4 ± 0.6, 8.3 ± 0.8, and 7.4 ± 1.0%, respectively (n = 5). The effects of BTC-δ4 and BTC were significant ($P < 0.05$) compared with saline-treated control. We also counted the number of apoptotic cells. On d 4, the number of TUNEL-positive cells was very low (less than $1 \times 10^{-6}/\mu m^2$).

Discussion

The present study was conducted to investigate the biological activity of the BTC splice variant, BTC-δ4. BTC-δ4 is unique in that it lacks the C-loop of the EGF motif and the transmembrane domain yet retains the signal peptide (15), suggesting that the protein produced from this transcript is a secreted protein. In contrast, BTC is synthesized as a transmembrane precursor, which can undergo 'ectodomain shedding' to release the soluble biologically active mature molecule. BTC-δ4 was found predominantly in the culture supernatant after expression in COS-7 cells as an approximately 14-kDa protein. In contrast, little, if any, BTC was found in the culture supernatant, the majority being present in the cell lysate (Fig. 2A) and on the cell surface (Fig. 2B). Thus, although BTC-δ4 is a protein product of the splicing variant of the BTC gene, the production of BTC-δ4 and BTC

TABLE 1. Characteristics of neonatal STZ-treated rats administered either BTC or BTC-δ4

	Normal	STZ	STZ/BTC-δ4	STZ/BTC
Body weight (g)	224 ± 12.0 (6)	212 ± 9.9 (5)	219 ± 8.4 (5)	220 ± 8.1 (5)
Pancreas weight (g)	0.80 ± 0.03 (6)	0.82 ± 0.06 (5)	0.91 ± 0.08 (5)	0.92 ± 0.06 (5)
Plasma glucose (mg/dl)	131.5 ± 6.0 (6)	160.0 ± 6.2 (5)	139.2 ± 3.4 (5)[a]	150.1 ± 5.3 (5)[b]
Plasma insulin (ng/ml)	2.8 ± 0.5 (6)	0.99 ± 0.3 (5)	1.92 ± 0.4 (5)[b]	1.14 ± 0.3 (5)
Insulin content (μg)	105.9 ± 5.2 (6)	39.0 ± 5.4 (5)	70.3 ± 5.5 (5)[a]	52.4 ± 5.5 (5)[b]
β-Cell mass (mg)	8.06 ± 0.70 (6)	2.40 ± 1.0 (5)	5.41 ± 0.8 (5)[a]	4.12 ± 0.9 (5)[b]

Data are mean ± SE (n). Neonatal STZ-treated rats were administered BTC, BTC-δ4, or saline, and various parameters were measured at 8 wk.

[a] $P < 0.01$ *vs.* the STZ group.

[b] $P < 0.05$ *vs.* the STZ group.

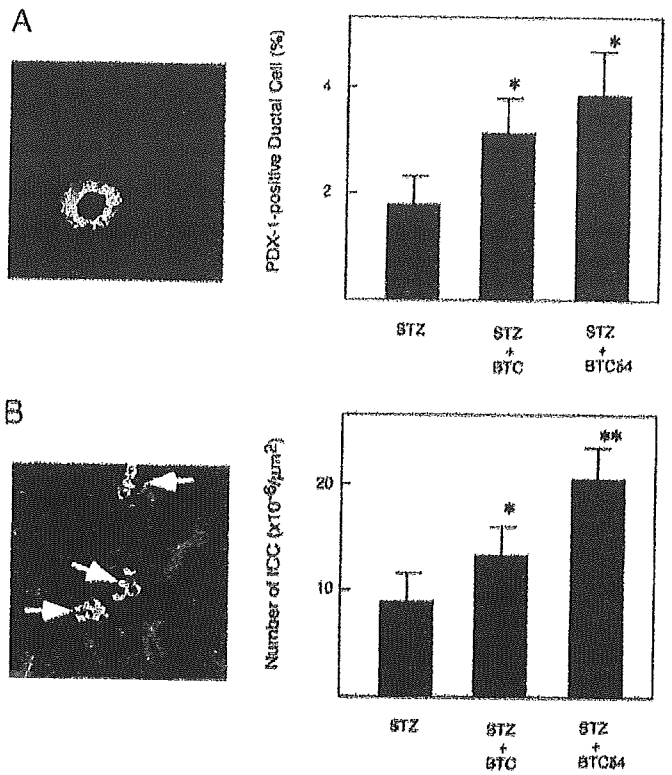

FIG. 8. Effect of BTC and BTC-δ4 on the numbers of PDX-1-positive cells and ICC. Rats were treated as indicated in the legend for Fig. 7, and the number of PDX-1-positive ductal cells (A) and ICC (B) were measured on d 4 in BTC- and BTC-δ4-treated rats. A, PDX-1-positive ductal cell; *red*, PDX-1; *green*, cytokeratin. B, ICC (indicated by the *arrow*); *red*, cytokeratin; *green*, insulin; *blue*, DAPI; STZ, STZ-injected rats treated with saline; *, $P < 0.05$ *vs.* STZ; **, $P < 0.01$ *vs.* STZ. Magnification, A, ×400; B, ×100.

is differentially regulated. The three disulfide loops and certain key residues in the two β-sheet structural regions of EGF ligands (for example, Gly49, Gly70, Arg72, and Leu78; Leu47 and Leu48 in EGF and TGF-α, respectively) are crucial for ErbB receptor binding (1, 2, 24). Because BTC-δ4 lacks the C-loop of the EGF motif encompassing Gly70, Arg72, and Leu78 (see Fig. 1), we were interested to determine whether BTC-δ4 was able to bind and activate ErbB-1 and ErbB-4, the principal BTC ErbB receptors (4, 5). BTC-δ4 was unable to bind or induce tyrosine phosphorylation of either ErbB-1 or ErbB-4 (Figs. 4 and 5), indicating that BTC-δ4 is not a ligand for either ErbB1 or ErbB4. Moreover, BTC-δ4 did not stimulate DNA synthesis in Balb/c 3T3 cells, which express ErbB-1 (Fig. 4), or induce phosphorylation of ErbB2/3 heterodimers (data not shown). In addition to stimulating cell proliferation, principally through ErbB1 and the activation of the Grb2-Sos-Ras-Raf-Mek1/2-Erk1/2 pathway, BTC also may act as a survival factor for various cell types through ErbB receptor-induced activation of the PI3K-Akt pathway (4, 5, 25). Consistent with this, we found that BTC, but not BTC-δ4, was able to inhibit apoptosis of AR42J-B20 cells induced by activin A (Fig. 6, E and F). These data support the concept that BTC-δ4 is not a ligand for the ErbB receptors and, hence, is unable to promote cell growth or survival. Nevertheless, both BTC and BTC-δ4 converted AR42J cells to insulin-producing cells (Fig. 6); and moreover, BTC-δ4 significantly increased the insulin content, β-cell mass, the number of PDX-1-positive ductal cells, and ICCs in neonatal STZ-treated rats (Table 1). Consequently, BTC-δ4 appears to act as a β-cell differentiation factor *in vitro* and *in vivo*, and it exerts this differentiation-inducing activity by acting through a unique cell surface receptor independent of either ErbB1 or ErbB4. We have previously postulated that BTC induces the differentiation of AR42J-B20 cells into insulin-secreting cells through a unique non-ErbB receptor of approximately 190 kDa (22). The data presented here strengthen this notion. Moreover, the fact that both BTC-δ4 and BTC display this differentiation-inducing activity suggests that the structural determinants for binding this unique receptor lie within the region Asp_{32}-Val_{94}. Analysis of C-terminal truncation derivatives of BTC, which display little affinity to ErbB1, are only weakly mitogenic for AR42J cells, yet retain the ability to induce the differentiation of these cells into insulin-secreting cells (26), is further consistent with this hypothesis. Taken together, these results suggest that the differentiation-inducing activity of both BTC and BTC-δ4 may be exerted through this unique receptor. The identification and characterization of this receptor is currently under investigation in our laboratory.

Previous studies have shown that BTC is able to increase the β-cell mass in various experimental rodent models of diabetes, indicating that it may represent a useful therapeutic approach for the treatment of the human condition (11–14). From a clinical point of view, administration of recombinant therapeutic growth factors to treat chronic disorders is hampered by the potential side effect of tumorigenesis, as a result of promoting cell proliferation. In this regard, because we have found that BTC-δ4 reproduces the differentiation activity of BTC without promoting cell proliferation, it may represent a more attractive therapeutic alternative for the treatment of diabetes. The observed *in vitro* apoptosis in cells treated with activin A and BTC-δ4 may not necessarily occur *in vivo* because β-cell progenitors would be bathed in a milieu of growth factors that may act to reduce apoptosis by virtue of their prosurvival properties. Thus, BTC-δ4 may be useful to treat certain types of diabetes caused by impaired β-cell neogenesis.

Acknowledgments

We thank Mayumi Odagiri for secretarial assistance during the preparation of the manuscript, and Ilka Priebe and Helen Webb for excellent technical assistance.

Received April 19, 2005. Accepted July 29, 2005.

Address all correspondence and requests for reprints to: Dr. Andrew J. Dunbar, GroPep Ltd., P.O. Box 10065 BC, Adelaide SA 5000, Australia. E-mail: andrew.dunbar@gropep.com.au; or Dr. Itaru Kojima, Institute for Molecular and Cellular Regulation, Gunma University, Maebashi 371-8512, Japan. E-mail: ikojima@showa.gunma-u.ac.jp.

This work was supported by a Grant-in-Aid for Scientific Research from the Ministry of Education, Science, Sports and Culture of Japan; a grant from the Project of Realization of Regeneration Medicine; and the Australian Government through the Cooperative Research Centres Programe.

References

1. Van Zoelen EJJ, Stortelers C, Lenferink AEG, Van de Poll MLM 2000 The EGF domain: requirements for binding to receptors of the ErbB family. Vitam Horm 59:99–131

2. **Harris RC, Chung E, Coffey RJ** 2003 EGF receptor ligands. Exp Cell Res 284:2–13
3. **van der Greer P, Hunter T, Lindberg RA** 1994 Receptor-tyrosine kinases and their signal transduction pathways. Annu Rev Cell Biol 10:251–337
4. **Alimandi M, Wang LM, Bottaro D, Lee CC, Kuo A, Frankel M, Fedi P, Tang C, Lippman M, Pierce JH** 1997 Epidermal growth factor and betacellulin mediate signal transduction through co-expressed ErbB2 and ErbB3 receptors. EMBO J 16:5608–5617
5. **Pinkas-Kramarski R, Leferink AEG, Bacus SS, Lyass L, an de Poll MLM, Klapper LN, Tzahar E, Sela M, van Zoelen EJJ, Yarden Y** 1998 The oncogenic ErbB2-ErbB-3 heterodimer is a surrogate receptor of the epidermal growth factor and betacellulin. Oncogene 16:1249–1258
6. **Shing Y, Christofori G, Hanahan D, Ono Y, Sasada R, Igarashi K, Folkman J** 1993 Betacellulin: a mitogen from pancreatic β cell tumors. Science 259:1604–1607
7. **Seno M, Tada H, Kosaka M, Sasada R, Igarashi K, Shing Y, Folkman J, Ueda M, Yamada H** 1996 Human betacellulin, a member of the EGF family, dominantly expressed in pancreas and small intestine, is fully active in a monomeric form. Growth Factors 13:181–191
8. **Miyagawa J, Hanafusa T, Sasada R, Yamamoto K, Igarashi K, Yamamoto K, Seno M, Tada R, Nammo T, Li M, Yamagata K, Nakajima H, Namba M, Kuwajima M, Matsuzawa Y** 1999 Immunohistochemical localization of pancreas and islet tumor cells. Endocr J 46:755–764
9. **Mashima H, Ohnishi H, Wakabayashi K, Miyagawa J, Hanafusa T, Seno M, Yamada H, Kojima I** 1996 Betacellulin and activin A coordinately convert amylase-secreting pancreatic AR42J cells into insulin-secreting cells. J Clin Invest 97:1647–1654
10. **Watada H, Kajimoto Y, Miyagawa J, Hanafusa T, Hamaguchi K, Matsuoka T, Yamamoto K, Matsuzawa Y, Kawamori R, Yamasaki Y** 1996 PDX-1 induces insulin and glucokinase gene expression in αTC clone 6 cells in the presence of betacellulin. Diabetes 45:1826–1831
11. **Yamamoto K, Miyagawa J, Waguri M, Sasada R, Igarashi K, Li M, Nammo T, Moriwaki T, Imagawa A, Yamagata K, Nakajima H, Namba M, Tochino Y, Hanafusa T, Matsuzawa Y** 2000 Recombinant betacellulin promotes neogenesis of β-cells and ameliorates glucose intolerance in mice with diabetes induced by selective alloxan perfusion. Diabetes 49:2021–2027
12. **Li L, Seno M, Yamada H, Kojima I** 2001 Promotion of β-cell regeneration by betacellulin in ninety percent pancreatectomized rats. Endocrinology 142:5379–5385
13. **Li L, Seno M, Yamada H, Kojima I** 2003 Betacellulin improves glucose metabolism by promoting conversion of intraislet precursor cells to β-cells in streptozotocin-treated mice. Am J Physiol 285:E577–E583
14. **Li L, Yi Z, Seno M, Kojima I** 2004 Activin A and betacellulin: effect on β-cell regeneration in neonatal streptozotocin-treated rats. Diabetes 53:608–615
15. **Dunbar A, Goddard C** 2000 Identification of an alternatively spliced mRNA branscript of human betacellulin lacking the C-loop of the EGF motif and the transmembrane domain. Growth Factors 18:169–176
16. **Loukianov E, Loukinanova T, Wiedlocha A, Olnes S** 1997 Expression of mRNA for a short form of heparin-binding EGF-like growth factor. Gene 195:81–86
17. **Maeda T, Kitazoe M, Tada H, de Llorens R, Salomon DS, Ueda M, Yamada H, Seno M** 2002 Growth inhibition of mammalian cells by eosinophil cationic protein. Eur J Biochem 269:307–316
18. **Dunbar AJ, Priebe IK, Belford DA, Goddard C** 1999 Identification of betacellulin as a major peptide growth factor in milk. Biochem J 344:713–721
19. **Tzahar E, Waterman H, Chen X, Levkowitz G, Karunagaran D, Lavi S, Ratzkin BJ, Yarden Y** 1996 A hierarchical network of interreceptor interactions determines signal transduction by Neu differentiation factor/neuregulin and epidermal growth factor. Mol Cell Biol 16:5276–5287
20. **Ogata T, Park KY, Seno M, Kojima I** 2004 Reversal of streptozotocin-induced hyperglycemia by transplantation of pseudoislets consisting of β-cells derived from ductal cells. Endocr J 51:381–386
21. **Carmichael J, DeGraff WC, Gazdar AF, Minnam JD, Mitchell JB** 1987 Evaluation of tetrazolium-based semiautomated colorimetric assay. Cancer Res 47:936–942
22. **Ishiyama N, Kanzaki M, Seno M, Yamada H, Kobayashi I, Kojima I** 1998 Studies in the betacellulin receptor in pancreatic AR42J cells. Diabetologia 41:623–628
23. **Furukawa M, Zhang YQ, Nie L, Shibata H, Kojima I** 1999 Role of MAP kinase and PI 3-kianse in differentiation of pancreatic AR42J cells induced by HGF. Diabetologia 42:450–456
24. **Groenen LC, Nice EC, Burgess AW** 1994 Structure-function relationships for the EGF/TGF-a family mitogens. Growth Factors 11:235–257
25. **Daly JM, Olayioye MA, Wong AM, Neve R, Lane HA, Maurer FG, Hynes NE** 1999 NDF/heregulin-induced cell cycle changes and apoptosis in breast tumor cells: role of PI3 kinase and p38 MAP kinase pathways. Oncogene 18:3440–3451
26. **Ito T, Kondo M, Tanaka Y, Kobayashi M, Sasada R, Igarashi K, Suenaga M, Koyama N, Nishimura O, Fujino M** 2001 Novel betacellulin derivatives. J Biol Chem 276:40698–40703

Endocrinology **is published monthly by The Endocrine Society (http://www.endo-society.org), the foremost professional society serving the endocrine community.**

J. Biochem. 137, 693–701 (2005)
DOI: 10.1093/jb/mvi081

Protein Transduction Assisted by Polyethylenimine-Cationized Carrier Proteins

Midori Kitazoe[1], Hitoshi Murata[1], Junichiro Futami[1,2], Takashi Maeda[1], Masakiyo Sakaguchi[3], Masahiro Miyazaki[3], Megumi Kosaka[1], Hiroko Tada[1], Masaharu Seno[1,4], Nam-ho Huh[3], Masayoshi Namba[5], Mitsuo Nishikawa[6], Yoshitake Maeda[6] and Hidenori Yamada[1,*]

[1]Department of Bioscience and Biotechnology, Faculty of Engineering, Graduate School of Natural Science and Technology, Okayama University, Okayama 700-8530; [2]Nippon Shokubai Co., Ltd.; [3]Department of Cell Biology, Okayama University Graduate School of Medicine and Dentistry, Okayama 700-8558; [4]Research Center for Biomedical Engineering, Okayama University, Okayama 700-8530; [5]Niimi College, Niimi, Okayama 718-8585; and [6]KIRIN Brewery Co., LTD, Pharmaceutical Division, Pharmaceutical Research Laboratories, Takasaki, Gunma 370-1295

Received January 6, 2005; accepted March 22, 2005

Previously, we have reported that cationized-proteins covalently modified with polyethylenimine (PEI) (direct PEI-cationization) efficiently enter cells and function in the cytosol [Futami *et al.* (2005) *J. Biosci. Bioeng.* 99, 95–103]. However, it may be more convenient if a protein could be delivered into cells just by mixing the protein with a PEI-cationized carrier protein having a specific affinity (indirect PEI-cationization). Thus, we prepared PEI-cationized avidin (PEI-avidin), streptavidin (PEI-streptavidin), and protein G (PEI-protein G), and examined whether they could deliver biotinylated proteins and antibodies into living cells. PEI-avidin (and/or PEI-streptavidin) carried biotinylated GFPs into various mammalian cells very efficiently. A GFP variant containing a nuclear localization signal was found to arrive even in the nucleus. The addition of a biotinylated RNase A derivative mixed with PEI-streptavidin to a culture medium of 3T3-SV-40 cells resulted in remarkable cell growth inhibition, suggesting that the biotinylated RNase A derivative entered cells and digested intracellular RNA molecules. Furthermore, the addition of a fluorescein-labeled anti-S100C (beta-actin binding protein) antibody mixed with PEI-protein G to human fibroblasts resulted in the appearance of a fluorescence image of actin-like filamentous structures in the cells. These results indicate that indirect PEI-cationization using non-covalent interaction is as effective as the direct PEI-cationization for the transduction of proteins into living cells and for expression of their functions in the cytosol. Thus, PEI-cationized proteins having a specific affinity for certain molecules such as PEI-streptavidin, PEI-avidin and PEI-protein G are concluded to be widely applicable protein transduction carrier molecules.

Key words: cationized carrier protein, protein G, polyethylenimine, protein transduction, streptavidin.

Abbreviations: CPP, cell-penetrating peptide; DMEM, Dulbecco's modified Eagle's medium; EDC, 1-ethyl-3-[3-(dimethylamino)propyl]carbodiimide hydrochloride; eGFP, enhanced green fluorescent protein; PEI, polyethylenimine; PTD, protein transduction domain; RITC, rhodamine B isothiocyanate; FITC, fluorescein isothiocyanate; FBS, fetal bovine serum; MTT, 3-(4,5-dimethylthiazol-2-yl)-2,5-diphenyltetrazolium bromide.

Protein delivery into living cells has been attracting a great deal of attention as a novel technology having potential both for basic research in cellular biology and for therapeutic application. Short basic peptides named protein transduction domains (PTD) or cell-penetrating peptides (CPP) have been found to deliver molecular cargo to target cells within the cytoplasm and/or nucleus of living cells. These peptides corresponding to the human immunodeficiency virus type 1 Tat-(48–60) (*1*, *2*), Antennapedia-(43–58) (*3*, *4*) and poly-Arg (*5*) are among the most well known PTD or CPP. By attaching these carrier peptides, efficient protein transduction of $p27^{Kip1}$ (*6*), p53 (*7*), Bcl-xL (*8*, *9*), Cre recombinase (*10*, *11*), and HOXB4 (*12*, *13*) was demonstrated to enable the modulation of cellular events *in vitro* and/or *in vivo*. The mechanism by which these cell-penetrating peptides (and their conjugates) enter cells has not yet been determined, but the electrostatic interaction between these peptides with polycationic charges and negatively charged proteoglycans on the cell surface is believed to trigger their efficient transduction (*14*, *15*).

As for protein cationization itself, it was proposed more than a decade ago that the method is applicable to intracellular protein delivery *via* adsorption-mediated endocytosis (*16*, *17*). The cationization of proteins is accomplished by extensive amidation of carboxyl groups with

*To whom correspondence should be addressed. Tel: +81-86-251-8215, Fax: +81-86-251-8265, E-mail: yamadah@cc.okayama-u.ac.jp

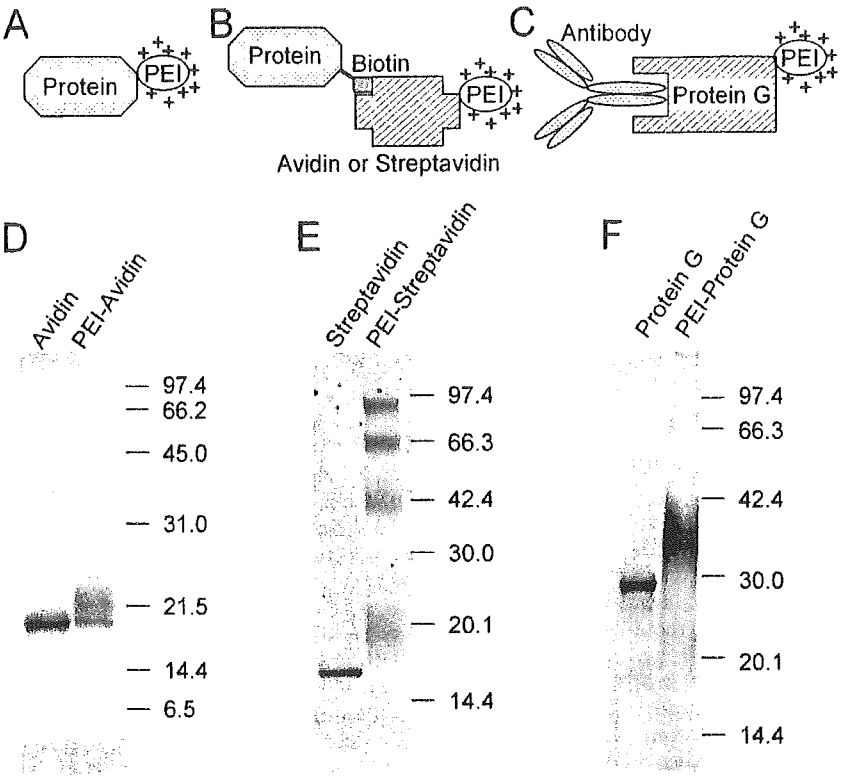

Fig. 1. **Schematic drawing of variously cationized proteins and SDS-PAGE analysis of native and chemically modified avidin, streptavidin, and protein G.** Protein cationized directly with PEI by carbodiimide reaction (A). Biotinylated protein complexed with PEI-avidin or PEI-streptavidin (B). Antibody bound to PEI-protein G (C). PEI-modification of avidin (D), streptavidin (E), and protein G (E) was analyzed by SDS-PAGE under reducing conditions in 15% (D), 15–25% gradient (E) and 10–20% gradient (F) polyacrylamide gels.

various diamines (*e.g.*, ethylenediamine). In fact, we have demonstrated that non-toxic secretory RNases become cytotoxic by cationization with ethylenediamine, indicating that they acquired a new function to pass through the cell membrane, although the cationized RNases showed considerably decreased enzymatic activity because of the modification of many carboxyl groups required for sufficient cationization (*18*). Thus, cationization is considered to be a powerful strategy for promoting cellular uptake of proteins. However, unfavorable effects on protein function and stability due to the extensive modification of carboxyl groups with diamines may limit its application (*19*).

Polyethylenimine (PEI) is a macromolecule with the highest cationic density among existing polycationic polymers. The modification of only a few residues with PEI (limited chemical conjugation) is needed for sufficient cationization to deliver proteins into living cells (Fig. 1A); therefore, the protein function can be maintained to a greater degree by limited PEI-cationization than by extensive diamine-cationization. Furthermore, PEI is toxicologically safe and has been used as a food additive, suggesting PEI to be a more suitable reagent than diamines for the cationization of proteins. In this context, we have demonstrated PEI-cationization to be an extremely useful method for protein transduction. Namely, we succeeded by using PEI-cationization to achieve efficient transduction of RNase A (expressing cytotoxicity), eGFP (intracellular fluorescence) (*20*) and anti-S100C (beta-actin binding protein) antibody (imaging of S100C along actin filaments and neutralization of S100C function) (*20*, *21*) into living cells. PEI-cationized proteins showed the ability to be transduced into living cells *in vitro* with 100% efficiency and at a substantially increased level compared with current PTD-fusion proteins (*20*). Therefore, PEI-cationization is considered to be an alternative and promising protein transduction method. However, the rather tedious chemical modification may limit its application. Thus, it may be more convenient if a protein could be delivered into cells just by mixing the protein with a PEI-cationized carrier protein having a specific affinity (indirect PEI-cationization) instead of by covalent modification with PEI (direct PEI-cationization; Fig. 1A). We describe here the utility of this 'PEI-cationized carrier protein method' for protein transduction into living cells using the following combinations as models: biotinylated GFP and biotinylated RNase A derivative with PEI-modified avidin or streptavidin (PEI-avidin or PEI-streptavidin, Fig. 1B) and anti-S100C antibody with PEI-modified protein G (PEI-protein G, Fig. 1C).

EXPERIMENTAL PROCEDURES

Materials—PEI (molecular mass 600) was purchased from Wako Chemicals (Osaka). 1-Ethyl-3-[3-(dimethylamino)propyl]carbodiimide hydrochloride (EDC) and Sulfo-NHS-SS-biotin was purchased from Pierce (Rockford, IL, USA). Bovine RNase A (Type XII-A), protein G and RITC-labeled rabbit anti-mouse IgG(H+L) polyclonal antibody (RITC–anti-mouse IgG) were obtained from Sigma (St. Louis, MO, USA). Biotin-AC_5-OSu was purchased from Dojindo (Kumamoto, Japan). Gradient polyacrylamide gel was purchased from Daiichi Pure Chemicals (Tokyo, Japan). An RNase A derivative (RNaseA-SO_3), in which the carboxyl groups of RNase A

were extensively amidated with taurine, was prepared as described previously (*18*). The preparation of rabbit antibody against human S100C was described previously (*22*). A complementary DNA of His-tagged eGFP, whose sequence has been reported previously (*6*), was subcloned into the pET14b vector (Novagen, WI, USA). A complementary DNA of GFPNuc, which encodes His-tagged eGFP with three copies of the nuclear localization signal (NLS) of the simian virus 40 large T-antigen fused at its C-terminus, was subcloned into the pET14b vector. The expression vector of His-tagged GFPUV5, a variant GFP with stronger fluorescence than eGFP, was kindly provided by Dr. M. Suzuki (*23*). These fusion proteins expressed in *Escherichia coli* BL21 (DE3) pLysS at 25°C were purified as described previously (*20*). Directly PEI-cationized eGFP was prepared by the carbodiimide reaction as described elsewhere (*20*).

PEI-Modification—Coupling reactions of proteins with PEI by EDC were carried out as described previously (*18*, *20*) in order to obtain PEI-cationized streptavidin (PEI-streptavidin), avidin (PEI-avidin) and protein G (PEI-protein G). The coupling conditions employed for each were as follows: streptavidin (0.1 mg/ml) in PEI-solution (60 mg/ml, pH 5) and 0.3 mg/ml EDC for 16 h at room temperature; avidin (2 mg/ml) in PEI-solution (100 mg/ml, pH 5) and 0.1 mg/ml for 1 h at room temperature; protein G (0.5 mg/ml) in PEI-solution (60 mg/ml, pH 5) and 1 mg/ml EDC for 16 h at 4°C. After the reaction, each solution except streptavidin was exhaustively dialyzed against PBS and stored at 4°C (avidin) or −20°C (protein G) until use. In the case of streptavidin, the solution was dialyzed against distilled water and then against 0.5 M hydroxylamine solution (pH 7.5). After 12-h dialysis against hydroxylamine, the solution was exhaustively dialyzed against distilled water and lyophilized. The lyophilized PEI-streptavidin was dissolved in PBS when it was used.

Biotinylation—Biotinylated eGFP (biotin-eGFP) or RNaseA-SO_3 (biotin-RNaseA-SO_3) was prepared by mixing a protein solution (pH adjusted to 9 with dilute NaOH) with Biotin-AC_5-OSu dissolved in dimethylformamide (DMF) at a molar ratio of the biotinylating reagent : protein of 2:1. GFPUV5 and GFPNuc were also biotinylated with Biotin-$(AC_5)_2$-OSu or Sulfo-NHS-SS-biotin in DMF at a molar ratio of the biotinylating reagent : protein of 5:1 to give biotin-GFPUV5 or biotin-SS-GFPUV5, and biotin-GFPNuc or biotin-SS-GFPNuc, respectively. After 2-h incubation at room temperature, the biotinylated proteins were purified by PD10 gel filtration (Amersham Bioscience, NJ, USA) using PBS as an elution buffer.

Cell Culture and Fluorescence Microscopy—BALB/c 3T3, 3T3-SV-40 (Dainippon Pharmaceutical Co., Tokyo), human fibroblasts OUMS-36 (*24*), HEK293 PEAK^{rapid} (Edge Biosystems, Gaithersburg, ML, USA), NIH-3T3, and HeLa S3 cells were cultured in Dulbecco's modified Eagle's medium (DMEM) supplemented with 10% fetal bovine serum (FBS) and 70 μg/ml of kanamycin. K562 cells were grown in RPMI1640 medium supplemented with 10% FBS and 70 μg/ml of kanamycin. Human fibroblasts (HFL-1) were cultured in Ham's F-12 medium supplemented with 15% FBS and 0.1 mg/ml streptomycin. Confocal microscopic analysis was performed by the following procedure. First, OUMS-36 or HFL-1 cells were grown in a glass-base dish in growth medium at 37°C until 50% confluent. Then the medium was changed to serum-free medium and protein samples were added to the medium. After 3-h incubation, the cells were washed several times with PBS and observed directly under a confocal laser-scanning microscope (model MRC-1024; Bio-Rad, CA, USA or model LSM 510; Carl Zeiss, Jena, Germany). In other cases, cells were grown on cover glasses in each growth medium at 37°C until 70% confluent. Then protein samples were added to the medium in the presence or absence of 10% FBS. After incubation for the indicated periods, the cells were washed several times with PBS and observed directly under a confocal laser-scanning microscope (model LSM 510; Carl Zeiss, Jena, Germany).

Flow Cytometry—Various exponentially growing cells were incubated with 100 nM of each of biotin-GFPUV5 and PEI-avidin that were premixed in the growth medium. After incubation for 24 h at 37°C, the cells were washed with PBS, dissociated with trypsin, and analyzed by fluorescence flow cytometry (FACSCalibur; Becton Dickinson, NJ, USA).

Cytotoxicity Assays—Cytotoxicity assays were conducted with 3T3-SV-40 cells. Cell viability was evaluated with 3-(4,5-dimethylthiazol-2-yl)-2,5-diphenyltetrazolium bromide (MTT; Sigma, MO, USA) as described previously (*25*, *26*) with some modification. Briefly, exponentially growing 3T3-SV-40 cells were seeded in a 96-well plate (4,000 cells/well) and incubated for 24 h at 37°C. The medium was replaced with serially diluted protein samples at the indicated concentrations (10 nM–1 μM) in serum-free medium. After 4-h cultivation, the medium was replaced with DMEM containing 10% FBS. Incubation was continued for 2 days before termination, and cell viability was determined using the MTT assay according to the manufacturer's instructions. The percent of cell growth was calculated in triplicate using cells grown without protein samples as a control.

RESULTS

Preparation of PEI-Carrier Proteins—Streptavidin, avidin and protein G were used as model carrier proteins for protein transduction. These proteins were cationized with PEI (average molecular mass 600) by a carbodiimide reaction under the conditions described in "EXPERIMENTAL PROCEDURES." To confirm PEI-modification, native and PEI-modified proteins were analyzed by SDS-PAGE. PEI-modified proteins gave bands that migrated more slowly and were broader in shape than the unmodified proteins (Fig. 1, D, E, and F). Avidin and streptavidin are both tetrameric proteins. In the case of PEI-avidin, about 2/3 of the monomer units (corresponding to 8/3 of a tetramer unit) seemed to be modified with PEI as judged from the ratio of unmodified monomer (Fig. 1D). On the other hand, PEI-streptavidin did not contain unmodified monomers, but contained non-dissociable dimers, trimers and tetramers in addition to modified monomers (Fig. 1E). These non-dissociable oligomers might be covalently cross-linked among intersubunits by the carbodiimide reaction. These results indicate that avidin, streptavidin and protein G were all successfully cationized with PEI, although avidin was somewhat lightly cationized. These

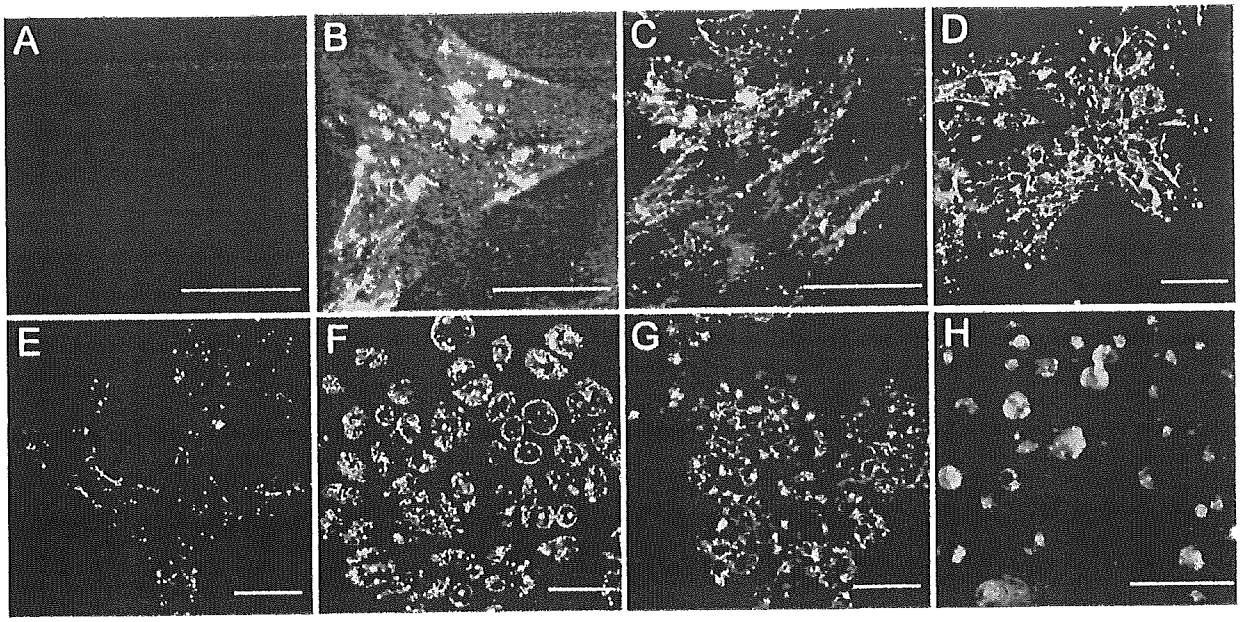

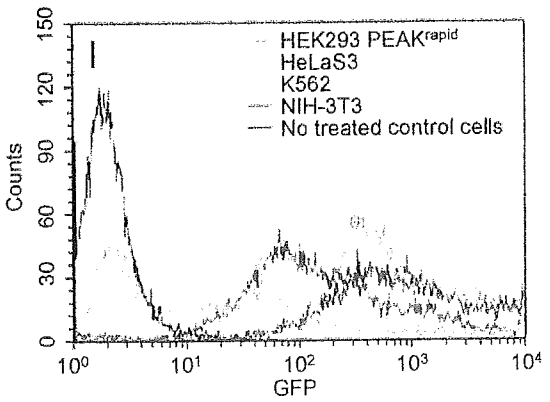

Fig. 2. **Intracellular delivery of biotinylated GFP variants with PEI-streptavidin or PEI-avidin.** Intracellular delivery of eGFP into human fibroblast OUMS-36 cells was analyzed by incubating of the cells with 250 nM biotin-eGFP and 125 nM streptavidin (A), with 250 nM biotin-eGFP and 125 nM PEI-streptavidin (B), and with 250 nM PEI-eGFP (C) for 3 h in the absence FBS. The other cells were treated with each protein sample for 2 h in the presence of 10% FBS. NIH-3T3 cells were treated with 100 nM biotin-GFPUV5 and 100 nM PEI-avidin (D), or 100 nM biotin-GFPUV5 and 100 nM avidin (E). HeLa S3 (F) and K562 (H) cells were treated with 100 nM biotin-GFPUV5 and 100 nM PEI-avidin. HEK293 PEAK^{rapid} cells were treated with 100 nM biotin-SS-GFPUV5 and 100 nM PEI-avidin (G). The cells were washed with PBS and examined under a confocal laser-scanning microscope [model MRC-1024; Bio-Rad (A–C), or model LSM 510; Carl Zeiss, Jena, Germany (D–H)]. The scale bars are equivalent to 50 μm. Transduction efficiency was also assessed by FACS analysis (I) (FACSCalibur; Becton Dickinson, NJ, USA). HEK293 PEAK^{rapid} (red), HeLa S3 (orange), K562 (green), and NIH-3T3 (blue) cells were treated with 100 nM of biotin-GFPUV5/PEI-avidin for 24 h in the presence of 10% FBS. One of the non-treated cells (HEK293 PEAK^{rapid}) is indicated by the black line as a representative.

PEI-modified proteins did not show any remarkable cytotoxicity toward tested mammalian cells at concentrations below 10 μM (data not shown), and were used as PEI-carrier proteins in this study.

Transduction of Biotinylated GFP with PEI-Streptavidin or with PEI-Avidin—The first model study of protein transduction assisted by PEI-cationized carrier protein was that using streptavidin-biotin or avidin–biotin interaction. eGFP variants were selected as model proteins to be delivered into cells because their cellular uptake can be monitored by fluorescence. Biotin-eGFP was mixed with PEI-streptavidin at a molar ratio of 1 to 2, and the mixture was added to a culture medium, serum-free DMEM, of OUMS-36 fibroblasts at a biotin-eGFP concentration of 250 nM. After incubation for 3 h at 37°C, the cells were washed with PBS and observed under a confocal laser-scanning microscope. The fluorescence of eGFP was clearly detected in these cells (Fig. 2B). There were no remarkable differences in the distributions and intensities of fluorescence of eGFP between cells treated with the biotin-eGFP/PEI-streptavidin complex (Fig. 2B) and those treated with directly PEI-cationized eGFP (PEI-eGFP, Fig. 2C). On the other hand, eGFP fluorescence could not be detected in cells treated with the biotin-eGFP/streptavidin (PEI-null) complex (Fig. 2A). These results indicate that in order to internalize proteins into living cells, indirect PEI-cationization using biotin-streptavidin interaction is as effective as direct PEI-cationization.

It has been previously reported that native avidin, which is a cationic protein having a net charge of +24 per tetramer at neutral pH, has the ability to introduce biotinylated peptides and antisense oligonucleotides into cells (27). However, PEI-cationized avidin (estimated net charge to be about +70 per tetramer) carries biotin-GFPUV5 into NIH-3T3 fibroblast cells much more efficiently than native avidin (Fig. 2, D and E), indicating that additional cationization of avidin does improve the transduction efficiency of biotinylated proteins. The transduction of biotinylated GFPUV5 (biotin-GFPUV5 or

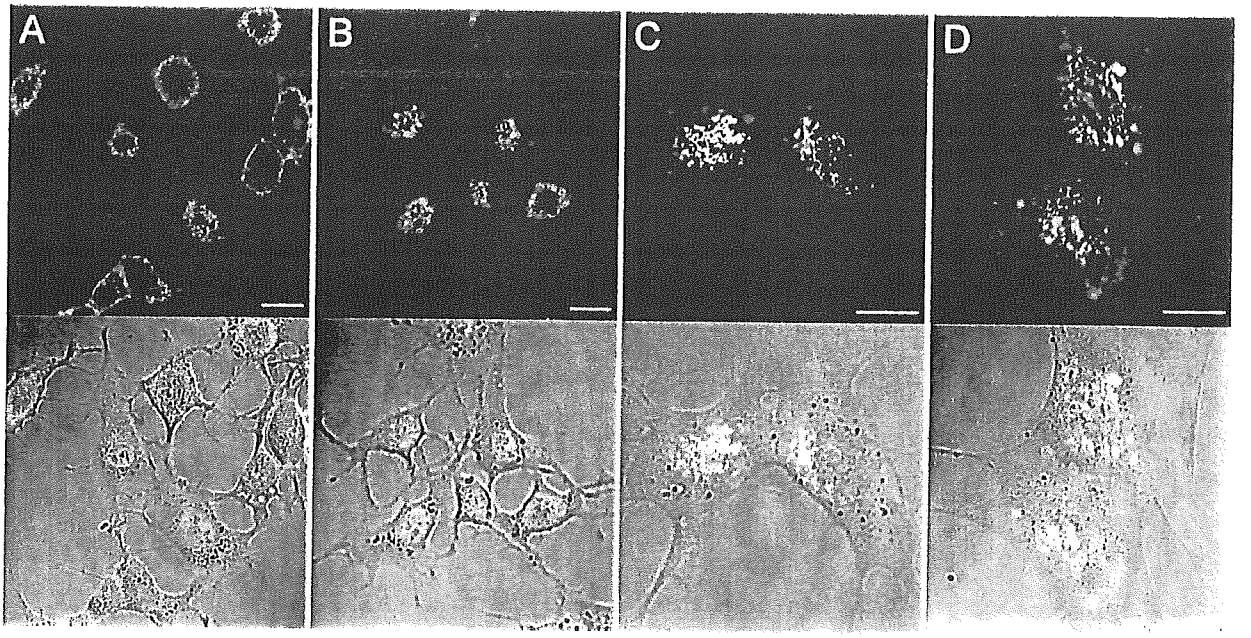

Fig. 3. **Confocal laser-scanning microscopy of cellular biotinylated GFPNuc fluorescence.** Intracellular delivery of GFP variants into Balb/c 3T3 cells was analyzed by incubatiing of the cells with 50 nM biotin-GFPUV5 and 50 nM PEI-avidin (A) and with 50 nM biotin-GFPNuc and 50 nM PEI-avidin (B) for 1 h in the absence FBS. Cells were treated with 100 nM biotin-GFPNuc and 100 nM PEI-avidin-RITC (C), or 100 nM biotin-SS-GFPNuc and 100 nM PEI-avidin-RITC (D) for 3 h in the absence of 10% FBS. The cells were washed with PBS, and examined under a confocal laser-scanning microscope (model LSM 510; Carl Zeiss, Jena, Germany). The scale bars are equivalent to 50 μm.

biotin-SS-GFPUV5) with PEI-avidin succeeded not only in fibroblast cell lines, but also in an epithelial cell line HeLa S3 (human cervical cancer cell line) (Fig. 2F), human embryonic kidney cell line HEK293 PEAK^{rapid} cells (Fig. 2G), and K562 (human chronic myelogenous leukemic cells) (Fig. 2H). Although biotin-SS-GFPUV5 contains a cleavable disulfide bond between the biotin moiety and the protein portion, Fig. 2G indicates that the cleavage of the disulfide bond did not occur outside the cells in the medium. FACS analysis revealed that biotinylated GFPUV5 was introduced with PEI-avidin into all of NIH-3T3 and HeLa S3 cells but only into about 65% of K562 cells (Fig. 2I).

Biotinylated GFP Fused with a Nuclear Localization Signal Sequence Was Carried into Cells by PEI-Avidin and Translocated into the Nucleus—Biotin-GFPUV5 transduced into NIH-3T3 cells by PEI-avidin produced granular fluorescence images around the inner rim of each cell (Fig. 3A). Fluorescence was hardly observed in nuclei. The granular images may indicate the partial localization of biotin-GFPUV5 in endocytic vesicles, as suggested previously that PEI-cationized proteins are internalized into cells mainly through an endocytic internalization pathway (*20*). On the other hand, biotin-GFPNuc, a biotinylated GFP derivative fused with three copies of the nuclear localization signal sequence (NLS) of the SV40 large T-antigen at the C-terminus, resulted in fluorescence in most nuclei (Fig. 3B). When biotin-GFPNuc was introduced into cells with rhodamine labeled PEI-avidin (PEI-avidin-RITC), green fluorescence due to GFP and red fluorescence due to RITC were co-localized in nuclei (Fig. 3C), suggesting that biotin-GFPNuc entered the nucleus as a complex with PEI-avidin-RITC. These results indicate that biotinylated proteins having NLS complexed with PEI-avidin entered not only endosomal vesicles but also the nucleus through the cytosol. Biotin-SS-GFPNuc, which has a cleavable disulfide bond between biotin and GFPNuc, was also introduced with PEI-avidin-RITC into cells. As shown in Figure 3D, green fluorescence from GFPNuc tended to appear in the nucleus while red fluorescence from PEI-avidin-RITC remained in the cyotosol. These results indicate that when a complex of biotin-SS-GFPNuc with PEI-avidin-RITC enters the cytosol, the disulfide bond is cleaved under the reducing environment causing the dissociation of GFPNuc from PEI-avidin-RITC, and GFPNuc portion is then further translocated into the nucleus.

RNase A Derivatives Carried to the Cytosol by PEI-Streptavidin Show Cytotoxicity—RNase A was selected as another model protein to be delivered into cells by indirect PEI-cationization using streptavidin-biotin interaction. We previously reported that RNaseA-SO_3, an RNase A derivative in which the carboxyl groups are extensively modified with taurine in amide bonds, acquires resistance to an RNase inhibitor and exhibits cytotoxicity by long-term exposure to cells due to endocytic leakage into the cells followed by cellular RNA degradation (*18*). Therefore, biotinylated RNaseA-SO_3 (biotin-RNaseA-SO_3) was prepared to examine whether PEI-streptavidin could intensify its cytotoxicity. 3T3-SV40 cells were cultured overnight at 37°C, and the medium was changed to serum-free DMEM. Biotin-RNaseA-SO_3 and PEI-streptavidin were mixed at a same molar ratio, and the mixture was added to the culture medium at biotin-RNaseA-SO_3–

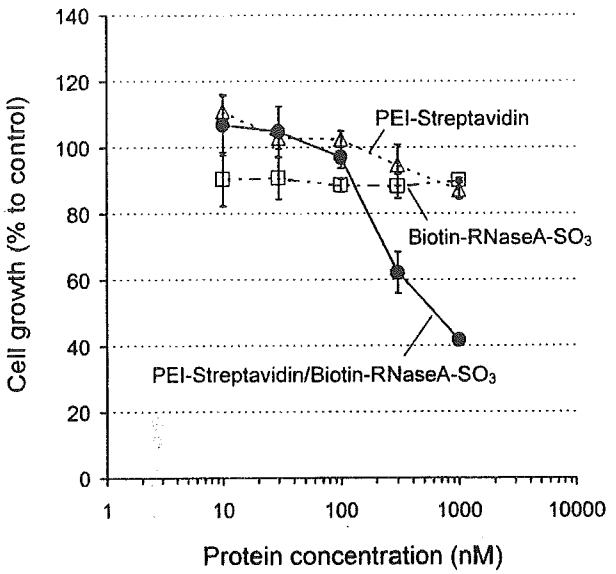

Fig. 4. **Cytotoxic activity of RNaseA-SO_3 introduced into cells using PEI-streptavidin carrier against 3T3-SV-40 cells.** 3T3-SV-40 cells in DMEM supplemented with 10% FBS were seeded into a 96-well plate (4000 cells/well), left to adhere for 24 h, and then treated with various concentrations of each protein sample in serum-free medium for 4 h. The culture medium has been replaced with DMEM containing 10% FBS, and the cells were cultured for 3 days before cell growth in each well was monitored by the MTT assay. Each value is the mean of three cultures, and is presented as a percentage of the value for buffer-treated cells, which is the mean value of the medium without protein sample.

based concentrations of 10 to 1,000 nM. After cultivation for 4 h, the medium was replaced with DMEM containing 10% FBS. The cells were cultured for another 2 days and then the viability of the cells was measured by MTT assay. As shown in Fig. 4, a dose-dependent cytotoxic effect of the biotin-RNaseA-SO_3/PEI-streptavidin complex was clearly observed (IC_{50} = 0.4 μM), while neither biotin-RNaseA-SO_3 nor PEI-streptavidin showed cytotoxic effects by themselves under the conditions employed. As mentioned before, PEI-carrier proteins, including PEI-streptavidin, do not show any remarkable cytotoxicity to the examined mammalian cells at concentrations below 10 μM. These results indicate that biotin-RNaseA-SO_3 is efficiently introduced into cells by the assistance of PEI-streptavidin and allowed to express RNase activity in cells resulting in the expression of cytotoxic activity.

Transduction of IgG Using PEI-Protein G—The second model study of protein transduction by indirect PEI-cationization was that using immunoglobulin-protein G interaction. An S100C protein belonging to the EF-hand Ca^{2+}-binding protein family was a key mediator of growth arrest (*21*). In a non-confluent state, S100C protein kept binding to actin filaments in normal human fibroblasts. Previously, we have reported that the FITC-labeled and directly PEI-cationized anti-S100C antibody enters cells producing fluorescence images of actin-like filamentous structures in human normal fibroblasts in a non-confluent state (*20*). Therefore, the anti-S100C antibody was selected as a model protein to be delivered into cells by PEI-protein G. The FITC-labeled anti-S100C antibody was mixed with PEI-protein G (1:1 molar ratio), and the mixture was added to the serum-free F-12 culture medium of human normal fibroblast HFL-1 cells at 100 nM. After 3-h cultivation, the cells were washed with PBS and observed under a confocal laser-scanning microscope. In addition to the fluorescence images of endosome-like granular structures, those of actin-like filamentous structures were observed in the cytoplasmic region (Fig. 5A). On the other hand, only granular structures were observed in cells treated with RITC-anti-mouse IgG/PEI-protein G complex (Fig. 5B). These results indicate that the PEI-protein G delivered the anti-S100C antibody into cells, which then at the right positions, that is, on S100C proteins bound to actin filaments.

DISCUSSION

We examined here the transduction efficiency of several proteins carried by PEI-cationized carrier proteins, PEI-streptavidin, PEI-avidin and PEI-protein G. When human OUMS-36 fibroblasts were incubated with the biotin-eGFP/PEI-streptavidin complex in serum-free DMEM, the cells exhibited granular fluorescence images in the cytoplasm rather than in the nuclei (Fig. 2B). Similar fluorescence images were observed in cells treated with eGFP cationized directly with PEI (Fig. 2C). Human HFL-1 normal fibroblasts treated with an RITC–anti-mouse IgG/PEI-protein G complex also gave similar granular fluorescence images in the cytoplasm (Fig. 4B). Furthermore, cells treated with RITC–anti-mouse IgG/PEI-cationized protein A, and those treated with a complex of RITC–anti-mouse IgG and PEI-cationized goat anti-mouse IgG also gave similar images (data not shown). On the other hand, no fluorescence was observed in cells treated with the biotin-eGFP/streptavidin (PEI-null) complex (Fig. 2A). PEI-avidin also effectively introduced biotin-GFPUV5 into cells (Fig. 2D) compared with avidin (PEI-null) (Fig. 2E). The transduction of biotinylated GFPUV5 with PEI-avidin was successful in all examined adhesive cell lines (Fig. 2, D, F, and G), although the efficiency differed depending on the cell line (Fig. 2I). Even in the case of a floating cell line, K562, biotin-GFPUV5 was introduced in about 65% of total cells by PEI-avidin (Fig. 2, H and I). Essentially, these PEI-carriers did not show any cytotoxicity at concentrations below 10 μM (data not shown). These results clearly indicate that the indirect cationization of proteins with PEI utilizing non-covalent intermolecular interactions, such as biotin-streptavidin, biotin-avidin, and antibody–protein G, as well as antibody-protein A and antigen-antibody, is as effective for protein transduction into living cells as direct cationization with PEI utilizing covalent conjugation.

In order to examine whether proteins thus internalized into cells could reach the cytosol and exhibit their functions inside cells, biotin-GFPNuc, biotin-RNaseA-SO_3 and FITC-labeled anti-S100C antibody were internalized into living cells by PEI-avidin, PEI-streptavidin and PEI-protein G, respectively. As a result, biotin-GFP-Nuc was imported into the nucleus (Fig. 3B), biotin-RNaseA-SO_3 expressed increased cytotoxicity due to the effective degradation of intracellular RNA molecules (Fig. 4), and FITC-labeled anti-S100C antibody revealed

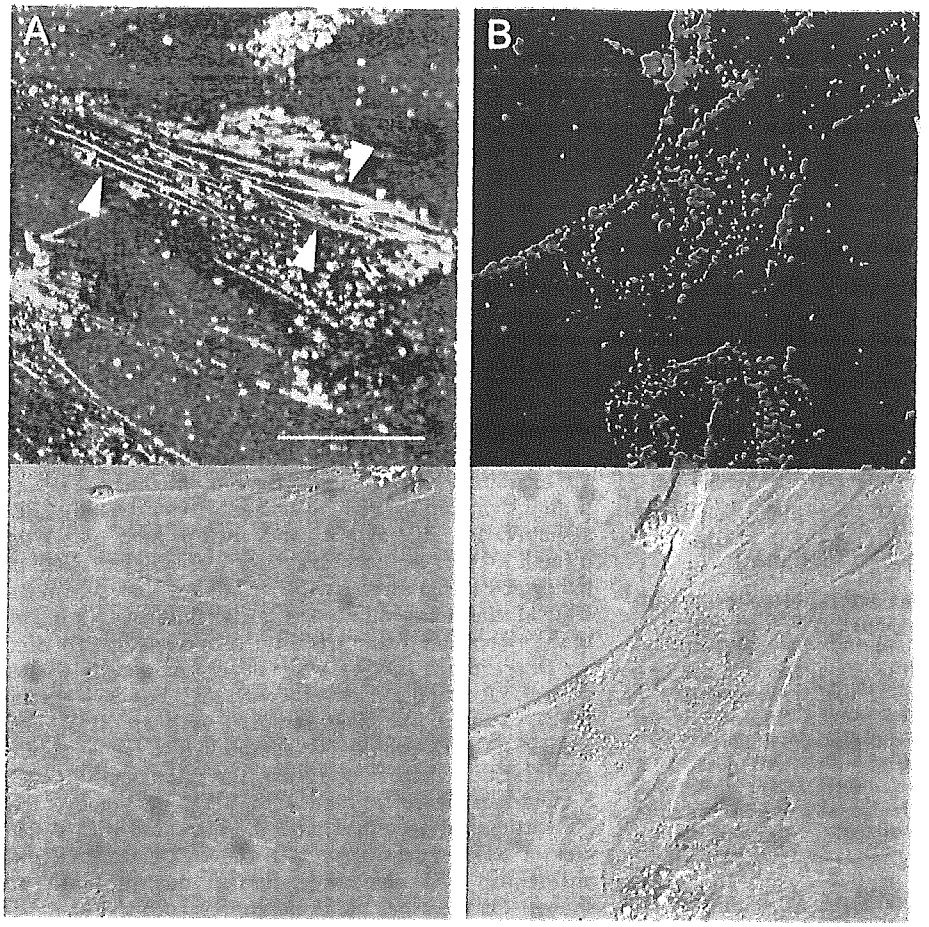

Fig. 5. **Confocal laser-scanning microscopy of the distribution of FITC-labeled anti-S100C antibodies introduced into cells by PEI-cationized protein G.** HFL-1 cells were grown in glass-base dishes in the presence of 15% FBS at 37°C until fifty percent confluent. Then the medium was replaced with serum-free medium and protein was added to the medium. After 3-h incubation, the cells were washed with PBS several times and analyzed directly under a confocal laser-scanning microscope (LSM 510; Carl Zeiss, Jena, Germany). When cells were treated with FITC–anti-S100C IgG/PEI-protein G complex, fluorescence was detected along with actin filaments (A), whereas no such specific fluorescence pattern was detected in cells treated with RITC–anti-mouse IgG/PEI-Protein G complex (B). Lower panels are differential interference contrast images corresponding to the upper panels. Arrowheads indicate filamentous structures. The scale bar is equivalent to 50 μm.

fluorescence images of filamentous structures due to binding to S100C proteins bound to actin filaments (Fig. 5A). All of these results clearly indicate that proteins internalized into living cells by indirect PEI-cationization can exhibit their functions inside cells as well as those internalized into cells by direct PEI-cationization.

Previously, we have demonstrated that PEI-cationization of proteins by direct modification with PEI is a very efficient method of protein transduction, and is, therefore, a very powerful tool for investigating cellular functions of proteins (*20*). In the present study, we succeeded in expanding of PEI-cationization to a method in which proteins to be delivered into living cells are PEI-cationized by "PEI-labeled carrier proteins." Once PEI-carrier proteins have been prepared, direct chemical modification with PEI of proteins to be delivered into cells is not necessary; only mixing the intact protein with its PEI-antibody, antibody with PEI-protein G or A, and biotinylated protein with PEI-streptavidin or PEI-avidin, is needed. Therefore, the tedious PEI modification step can be avoided. This methodology will also be effective if there are many proteins to be examined, such as in the case of screening the cellular functions of numerous proteins. For example, using PEI-streptavidin or PEI-avidin as a carrier protein, any biotinylated protein can be internalized into cells. Biotinylation is one of the most-extensively studied chemical modifications and many kinds of biotinylating reagents are currently available. Therefore, biotinylation may be easier and safer with regard to the risks of conformational change and loss of function of a protein than direct PEI-modification. Besides chemical modification, sequence-specific biotinylation with biotin holozyme synthetase is also available by co-expression of proteins with the biotinylation sequence and enzyme using an *E. coli.* expression system (*28*). PEI-protein G and PEI-protein A make it possible to internalize valuable and rare antibodies into living cells. This method may be used for the neutralization of intracellular protein function if a neutralizing antibody is available.

Disulfide bonds can be cleavaged under the reductive environment of the cytosol. Therefore, by using biotinylating reagents having disulfide bonds, a protein delivered into cells would become free from the PEI-carrier protein in the cytosol. In fact, the transduction of biotin-SS-GFPNuc with PEI-avidin resulted in the dissociation of GFPNuc from PEI-avidin within cells (Fig. 3D). This type of biotinylating reagent may be effective for the transduction of a protein if cationic modification interferes with the protein function.

A previous report suggested that native avidin has the ability to introduce peptides and antisense oligonucleotides into cells (*27*). However, as shown in Fig. 2, D and E, PEI-avidin is highly superior to intact avidin. It has also been reported that a fluorescence-labeled antibody

can be introduced into cells using TAT-protein A as a carrier in which protein A is genetically fused with the TAT peptide (*29*). However, the expression of the functions of the proteins transduced into cells by these carrier proteins was not clear in either report. Therefore, this is the first report of proteins introduced by carrier proteins reaching the cytosol and expressing their function inside cells: RNase activity, transport to the nucleus, and recognition of antigen S100C.

In addition to filamentous images, granular fluorescence images were observed in cells treated with either PEI–anti-S100C antibody (*20*) or anti-S100C antibody/PEI-protein G complex (Fig. 5A). PTD- or CPP-fused proteins mediate cell surface adhesion, which is followed by internalization into cells by endocytosis, and fluorescence-labeled TAT-fusion proteins localize in endocytic vesicles (*11, 30*). We have also reported that PEI-cationized eGFP is internalized through an endocytic internalization pathway (*20*). The granular fluorescence images suggest the partial localization of excess PEI–anti-S100C or anti-S100C antibody/PEI-protein G complex in endocytic vesicles. Otherwise, the anti-S100C antibody used here contained non-specific IgGs. For live cell imaging of intracellular proteins, these granular fluorescence images are not preferable. Therefore, part of the future research will seek to reduce these granular fluorescence images.

In conclusion, the "PEI-cationized carrier method" developed here is a simple and widely applicable protein transduction method, and is expected to serve as a potential tool for basic research in cellular biology and for therapeutic applications

We would like to express thanks to Dr. M. Suzuki for the His-tagged GFPUV5 vector. This work was performed as a part of a research and development project of the Industrial Science and Technology Program supported by the New Energy and Industrial Technology Development Organization (NEDO).

REFERENCES

1. Vivès, E., Brodin, P., and Lebleu, B. (1997) A truncated HIV-1 Tat protein basic domain rapidly translocates through the plasma membrane and accumulates in the cell nucleus. *J. Biol. Chem.* **272**, 16010–16017
2. Schwarze, S.R., Ho, A., Vocero-Akbani, A., and Dowdy, S.F., (1999) *In vivo* protein transduction: delivery of a biologically active protein into the mouse. *Science* **285**, 1569–1572
3. Derossi, D., Joliot, A.H., Chassaing, G., and Prochiantz, A. (1994) The third helix of the Antennapedia homeodomain translocates through biological membranes. *J. Biol. Chem.* **269**, 10444–10450
4. Derossi, D., Chassaing, G., and Prochiantz, A. (1998) Trojan peptides: the penetratin system for intracellular delivery. *Trends Cell Biol.* **8**, 84–87.
5. Futaki, S., Nakase, I., Suzuki, T., Youjun, Z., and Sugiura, Y. (2002) Translocation of branched-chain arginine peptides through cell membranes: flexibility in the spatial disposition of positive charges in membrane-permeable peptides. *Biochemistry* **41**, 7925–7930
6. Nagahara, H., Vocero-Akbani, A.M., Snyder, E.L., Ho, A., Latham, D.G., Lissy, N.A., Becker-Hapak, M., Ezhevsky, S.A., and Dowdy, S.F. (1998) Transduction of full-length TAT fusion proteins into mammalian cells: TAT-p27Kip1 induces cell migration. *Nat. Med.* **4**, 1449–1452
7. Takenobu, T., Tomizawa, K., Matsushita, M., Li, S.T., Moriwaki, A., Lu, Y.F., and Matsui, H. (2002) Development of p53 protein transduction therapy using membrane-permeable peptides and the application to oral cancer cells. *Mol. Cancer Ther.* **1**, 1043–1049
8. Cao, G., Pei, W., Ge, H., Liang, Q., Luo, Y., Sharp, F.R., Lu, A., Ran, R., Graham, S.H., and Chen, J. (2002) *In Vivo* Delivery of a Bcl-xL Fusion Protein Containing the TAT Protein Transduction Domain Protects against Ischemic Brain Injury and Neuronal Apoptosis. *J. Neurosci.* **22**, 5423–5431
9. Asoh, S., Ohsawa, I., Mori, T., Katsura, K., Hiraide, T., Katayama, Y., Kimura, M., Ozaki, D., Yamagata, K., and Ohta, S. (2002) Protection against ischemic brain injury by protein therapeutics. *Proc. Natl. Acad. Sci. USA* **99**, 17107–17112
10. Peitz, M., Pfannkuche, K., Rajewsky, K., and Edenhofer, F. (2002) Ability of the hydrophobic FGF and basic TAT peptides to promote cellular uptake of recombinant Cre recombinase: a tool for efficient genetic engineering of mammalian genomes. *Proc. Natl. Acad. Sci. USA* **99**, 4489–4494
11. Wadia, J.S., Stan, R.V., and Dowdy, S.F. (2004) Transducible TAT-HA fusogenic peptide enhances escape of TAT-fusion proteins after lipid raft macropinocytosis. *Nat. Med.* **10**, 310–315
12. Krosl, J., Austin, P., Beslu, N., Kroon, E., Humphries, R.K., and Sauvageau, G. (2003) *In vitro* expansion of hematopoietic stem cells by recombinant TAT-HOXB4 protein. *Nat. Med.* **9**, 1428–1432
13. Amsellem, S., Pflumio, F., Bardinet, D., Izac, B., Charneau, P., Romeo, P.H., Dubart-Kupperschmitt, A., and Fichelson, S., (2003) Ex vivo expansion of human hematopoietic stem cells by direct delivery of the HOXB4 homeoprotein. *Nat. Med.* **9**, 1423–1427
14. Rusnati, M., Tulipano, G., Spillmann, D., Tanghetti, E., Oreste, P., Zoppetti, G., Giacca, M., and Presta, M. (1999) Multiple interactions of HIV-I Tat protein with size-defined heparin oligosaccharides. *J. Biol. Chem.* **274**, 28198–28205
15. Tyagi, M., Rusnati, M., Presta, M., and Giacca, M. (2001) Internalization of HIV-1 tat requires cell surface heparan sulfate proteoglycans. *J. Biol. Chem.* **276**, 3254–3261
16. Kumagai, A.K., Eisenberg, J.B., and Pardridge, W.M. (1987) Absorptive-mediated endocytosis of cationized albumin and a beta-endorphin-cationized albumin chimeric peptide by isolated brain capillaries. Model system of blood-brain barrier transport, *J. Biol. Chem.* **262**, 15214–15219
17. Apple, R.J., Domen, P.L., Muckerheide, A., and Michael, J.G. (1988) Cationization of protein antigens. IV. Increased antigen uptake by antigen-presenting cells, *J. Immunol.* **140**, 3290–3295
18. Futami, J., Maeda, T., Kitazoe, M., Nukui, E., Tada, H., Seno, M., Kosaka, M., and Yamada, H. (2001) Preparation of potent cytotoxic ribonucleases by cationization: enhanced cellular uptake and decreased interaction with ribonuclease inhibitor by chemical modification of carboxyl groups. *Biochemistry* **40**, 7518–7524
19. Futami, J., Nukui, E., Maeda, T., Kosaka, M., Tada, H., Seno, M., and Yamada, H. (2002) Optimum modification for the highest cytotoxicity of cationized ribonuclease. *J. Biochem.* **132**, 223–228
20. Futami, J., Kitazoe, M., Maeda, T., Nukui, E., Sakaguchi, M., Kosaka, J., Miyazaki, M., Kosaka, M., Tada, H., Seno, M., Sasaki, J., Huh, N.H., Namba, M., and Yamada, H. (2005) Intracellular Delivery of Proteins into Mammalian Living Cells by Polyethylenimine-Cationization. *J. Biosci. Bioeng.* **99**, 95–103
21. Sakaguchi, M., Miyazaki, M., Takaishi, M., Sakaguchi, Y., Makino, E., Kataoka, N., Yamada, H., Namba, M., and Huh, N.H. (2003) S100C/A11 is a key mediator of Ca^{2+}-induced growth inhibition of human epidermal keratinocytes. *J. Cell Biol.* **163**, 825–835
22. Sakaguchi, M., Miyazaki, M., Inoue, Y., Tsuji, T., Kouchi, H., Tanaka, T., Yamada, H., and Namba, M. (2000) Relationship between contact inhibition and intranuclear S100C of normal human fibroblasts. *J. Cell Biol.* **149**, 1193–1206

23. Suzuki, M., Ito, Y., Savage, H.E., Husimi, Y., and Douglas, K.T. (2004) Protease-sensitive signalling by chemically engineered intramolecular fluorescence resonance energy transfer mutants of green fluorescent protein. *Biochim. Biophys. Acta* **1679**, 222–229
24. Namba, M., Nishitani, K., Hyodoh, F., Fukushima, F., and Kimoto, T. (1985) Neoplastic transformation of human diploid fibroblasts (KMST-6) by treatment with 60Co gamma rays. *Int. J. Cancer* **35**, 275–280
25. Tada, H., Shiho, O., Kuroshima, K., Koyama, M., and Tsukamoto, K. (1986) An improved colorimetric assay for interleukin 2. *J. Immunol. Methods* **93**, 157–165
26. Futami, J., Seno, M., Ueda, M., Tada, H., and Yamada, H. (1999) Inhibition of cell growth by a fused protein of human ribonuclease 1 and human basic fibroblast growth factor. *Protein Eng.* **12**, 1013–1019
27. Pardridge, W.M. and Boado, R.J. (1991) Enhanced cellular uptake of biotinylated antisense oligonucleotide or peptide mediated by avidin, a cationic protein. *FEBS Lett.* **288**, 30–32
28. Chapman-Smith, A. and Cronan, J.E., Jr. (1999) The enzymatic biotinylation of proteins: a post-translational modification of exceptional specificity. *Trends Biochem. Sci.* **24**, 359–363
29. Mie, M., Takahashi, F., Funabashi, H., Yanagida, Y., Aizawa, M., and Kobatake, E. (2003) Intracellular delivery of antibodies using TAT fusion protein A. *Biochem. Biophys. Res. Commun.* **310**, 730–734
30. Richard, J.P., Melikov, K., Vives, E., Ramos, C., Verbeure, B., Gait, M.J., Chernomordik, L.V., and Lebleu, B. (2003) Cell-penetrating peptides. A reevaluation of the mechanism of cellular uptake, *J. Biol. Chem.* **278**, 585–590

Protein Engineering, Design & Selection vol. 18 no. 7 pp. 321–327, 2005
Published online June 24, 2005 doi:10.1093/protein/gzi040

Anti-angiogenic effect of an insertional fusion protein of human basic fibroblast growth factor and ribonuclease-1

Tetsu Hayashida[1], Masakazu Ueda[1,2], Koichi Aiura[1], Hiroko Tada[3], Masayuki Onizuka[3], Masaharu Seno[3], Hidenori Yamada[3] and Masaki Kitajima[1]

[1]Department of Surgery, School of Medicine, Keio University, Shinanomachi 35, Shinjyuku-ku, Tokyo 160-8582 and [3]Department of Bioscience and Biotechnology, Faculty of Engineering, Graduate School of Natural Science and Technology, Okayama University, Okayama 700-8530, Japan

[2]To whom correspondence should be addressed.
E-mail: m_ueda@sc.itc.keio.ac.jp

Human pancreatic ribonuclease-1 (RNase1) does not exhibit its cytotoxicity unless it is artificially internalized into the cytosol. Furthermore, once it encounters the cytosolic RNase inhibitor (RI), the activity of RNase1 is seriously reduced. To achieve the cellular targeting of RNase1 and the blocking of RI binding simultaneously, the basic fibroblast growth factor (bFGF) sequence was inserted into RNase1 at the RI binding site using a gene fusion technique. The effect of this fusion protein, CL-RFN89, on the angiogenesis, which was accelerated by FGF–FGF receptor interaction, was investigated. It was shown by using fluorescein-labeled CL-RFN89, that the binding to human umbilical vein endothelial cells (HUVECs) was dependent on the existence of the FGF receptors. In addition, CL-RFN89 inhibited the cellular growth of HUVECs *in vitro* and also inhibited the tube formation, using a three-dimensional tube formation assay. Furthermore, this fusion protein was shown to prevent *in vivo* tumor cell-induced angiogenesis, using the mouse dorsal air sac assay. These results demonstrated that CL-RFN89 inhibits angiogenesis *in vitro* and *in vivo* and that it can be expected to be a potent antiangiogenic agent.
Keywords: angiogenesis/basic fibroblast growth factor/fusion protein/molecular targeting/ribonuclease

Introduction

Angiogenesis is necessary for the neoplasm to grow beyond 1–2 mm in diameter and for tumor metastasis (Folkman and Shing, 1992). Underlying angiogenesis are a series of complex processes, such as degradation of the extracellular matrix, migration, proliferation and maturation of the endothelial cells (Risau, 1997). This process is a characteristic feature not only of aggressive solid tumors, but also of other diseases, such as rheumatoid arthritis, psoriasis and ocular disorders, including the exudative form of age-related macular degeneration and diabetic retinopathy (Folkman, 1992; O'Reilly *et al.*, 1996, 1997). Angiogenesis is a rare phenomenon in health adults. It occurs only locally and transiently under distinctive physiological conditions, such as wound healing, inflammation and the female reproductive cycle. Inhibition of the angiogenic process has been to become one of the most promising strategies for the treatment of malignant neoplasms and the above-mentioned disorders.

Various antiangiogenic agents have been identified and some of these are currently under clinical trials (Karp *et al.*, 1995). Most of these inhibitors of angiogenesis, however, pose problems in therapeutic application because of their excessive toxicity and limited efficacy. To resolve these problems, a variety of studies on molecular targeting chemotherapy for neoplasms have been reported, since this might allow higher specificity and reduced systemic toxicity. Several angiogenic factors have been identified and investigated, but vascular endothelial growth factor (VEGF) and fibroblast growth factor (FGF) have perhaps been the most studied (Li, 2000). FGF is a potent pleiotropic heparin-binding mitogen for vascular endothelial cells. It acts synergistically with VEGF to stimulate new vessel growth (de Jong *et al.*, 1998; Seghezzi *et al.*, 1998; Klint *et al.*, 1999; Giavazzi *et al.*, 2001). Therefore, targeting FGF or FGF receptors in order to achieve angiogenesis inhibition can be a strategy for therapy. For example, antiangiogenic platelet factor-4 (PF-4) fragments associate with FGF and impair cell-surface receptor binding to inhibit angiogenesis *in vivo* (Hagedorn *et al.*, 2001). Treatment of tumors with three tyrosine kinase receptors, including the FGF receptor, markedly suppressed tumor growth and decreased tumor blood flow (Griffin *et al.*, 2002).

Recently, we designed a fusion protein, composed of human RNase1, which was cloned from human pancreas and human bFGF and reported that this protein exerted cell type-specific growth inhibition against malignant cells bearing FGF receptors (Futami *et al.*, 1995, 1999). RNase–FGF fusion proteins are considered to be effectively internalized into the cytosol via the FGF receptors. As a result, they degrade cellular RNA and inhibit protein synthesis.

In a previous study, the generation of an end-to-end fusion protein between RNase1 and bFGF by simple gene linkage was explored. This protein was designed to evade the effect of ribonuclease inhibitor protein (RI) by truncation of seven amino acid residues in the N-terminal sequence of RNase1. Nevertheless, through this method, the protein function could not be demonstrated adequately nor could the stability of the fusion protein be established, because it was difficult to control the configuration between these proteins and choices of the stereostructure were limited. Therefore, we attempted to construct a new concept of fusion protein, by which a domain of the second protein was inserted genetically into the first protein. In this method, the position of the inserted domain could be varied to obtain various protein stereostructures. Thus, to achieve the blocking of RI binding and cellular targeting of RNase simultaneously, bFGF was inserted genetically into Gly89 of RNase1 (RI bindng site of RNase1) to prevent from its stereostructural binding to RI. The resultant protein, CL-RFN89, had abilities both for efficient binding to target cells and for evading RI by masking the RI interaction site with the targeting protein of bFGF. CL-RFN89 retained its activity at >85% even in the presence of a 200-fold molar excess of

RI and showed a growth inhibitory effect on mouse B16/BL6 melanoma cells (Tada *et al.*, 2004), which expresses both bFGF and high-affinity FGF receptor (Blanckaert *et al.*, 1993). Subsequently, tumor angiogenesis that is mediated and promoted by the FGF–FGF receptor interaction is assumed to be suppressed by this fusion protein.

In this study, the effect of CL-RFN89 on the antiangiogenic response was investigated, in both *in vitro* and *in vivo* angiogenesis models. Furthermore, the possibility of CL-RFN89, reacting with the vascular endothelial cells specifically through FGF receptors was also examined.

Materials and methods

Reagents

Dulbecco's modified Eagle's medium (DMEM) and phosphate-buffered saline (PBS) were obtained from Sigma Chemical (St Louis, MO). Fetal bovine serum (FBS) was obtained from JRH Bioscience (Lenexa, KS). Recombinant human fibroblast growth factor-basic was purchased from Pepro Tech EC (London, UK). The EGM bullet-kit (containing endothelial basal medium, hEGF, hydrocortisone, BBE, FBS and GA-1000), trypsin, cell matrix-type I-A, MCDB131 and gel reconstruction buffer were supplied by Asahi Techno Glass (Chiba, Japan). A fluorescein labeling kit was obtained from Roche Diagnostics (Mannheim, Germany). Cell Counting Kit-8, nembutal and diethyl ether were obtained from Wako Pure Chemical Industries (Osaka, Japan). A Millipore chamber (diameter, 14 mm; thickness, 2 mm) and membrane filter (diameter, 13 mm; thickness, 180 μm; filter pore size, 0.45 μm) were obtained from Millipore (Bedford, MA). Six and 24 multi-well plates were purchased from Sumitomo Bakelite (Tokyo, Japan).

Cell lines

A431 cells procured from Riken (Saitama, Japan) were maintained in DMEM containing 10% FBS. Human umbilical vein endothelial cells were procured from Asahi Techno Glass and cultured in EGM containing 2% FBS. All the cells were cultured in an atmosphere of 5% CO_2 at 37°C.

Animals

Female 6-week-old BALB/c mice obtained from CLEA Japan (Tokyo, Japan) were used. The animals were housed in an air-conditioned room at 22–23°C, with free access to food and water.

Construction of CL-RFN89

The methods of construction and purification of insertional fusion protein, CL-RFN89, were described previously (Tada *et al.*, 2004). To summarize them briefly, recombinant human 4–118 cross-linked RNase1(CL-RNase1) and human bFGF (147 amino acid form) were purified from *Escherichia coli* (Futami *et al.*, 1999, 2000a). A cDNA encoding bFGF(19–146) (N-terminal 18 residue-truncated form of bFGF) was amplified by polymerase chain reaction. A *Sac*II site was introduced at the position of Gly89 of CL-RNase1 cDNA into a CL-RNase1 expression vector. The resultant plasmids were cleaved with *Sac*II and ligated in frame with the *Sac*II fragment of bFGF(19–146) to construct the expression vectors for insertional-fusion proteins (Futami *et al.*, 2000b). The recombinant proteins were expressed as inclusion bodies in *E.coli* and then solubilized and refolded (Futami *et al.*, 1995). The refolded proteins were purified by cation-exchange chromatography. The main peak fractions were collected and concentrated by ultrafiltration.

Binding assay

Fluorescein-labeled CL-RFN89 was synthesized by coupling 5(6)-carboxyfluorescein-*N*-hydroxysuccinimide ester (FLUOS) to the amino groups of CL-RFN89 using the fluorescein labeling kit, according to the manufacturer's instructions. To explain briefly, 1 mg of CL-RFN89 dissolved in PBS was incubated with 0.14 mg of FLUOS dissolved in 100% DMSO for 2 h at room temperature, with gentle mixing. Unbound FLUOS was removed by Sephadex G-25 gel filtration. The approximate fluorescein to protein ratio was 5:1.

The binding assay was performed to confirm whether the effect of CL-RFN89 was mediated through the FGF receptor. A total of 1×10^5 cells of HUVECs were suspended in phosphate-buffered saline and the cell suspension was mixed with fluorescein-labeled CL-RFN89 to obtain a solution of 2 μM concentration. The cells were washed twice with PBS at 4°C after 15 min of incubation and then examined under a fluorescence microscope (ECLIPSE E1000, Nikon, Tokyo, Japan). An excess amount of human recombinant bFGF was used to investigate the competitive inhibition of FGF receptors by CL-RFN89. Before incubation was started, the cells and the fluorescein-labeled protein complex were treated with 30 μM bFGF. They were also incubated, washed and observed in a similar manner. These experiments were performed in triplicate.

In vitro angiogenesis assay

Tube formation of HUVECs in a type I collagen gel was analyzed as the assay of angiogenesis *in vitro*. For the preparation of the collagen gel, 8 volumes of Cellmatrix Type I-A (3.0 mg/ml) were mixed with 1 volume of 10× MCDB131 and 1 volume of gel reconstruction buffer (50 mM sodium hydroxide, 260 mM sodium hydrogen carbonate, 200 mM HEPES). A 1 ml volume of the mixture was added at 4°C to each well of the multi-well plate (six wells; 38 mm diameter) and the gel was incubated at 37°C for at least 30 min, to allow for gelation. The gel was covered with 1 ml of a similar collagen gel after HUVECs were plated on the gel at a concentration of 1.5×10^5 cells and incubated in EGM at 37°C for 4 h. The cells were then exposed to various concentrations of reagents added to EGM. After incubation for 48 h, fields of tube-like structures that formed in the gel were observed at random under an optical microscope and the total lengths per field (×40) were measured by computer image analysis (Scion Image, version 0.4.0.2, Scion, Maryland). All the experiments were performed three times and the results were expressed as means and standard deviations.

Cytotoxicity of CL-RFN89 against A431 cells and HUVECs

CL-RFN89 was added to a 96-well plate containing the cells at a density of 10^4 cells in 100 μl of DMEM per well and then cultured to assess its cytotoxicity against A431 cells and HUVECs. After 48 h of incubation with various concentrations of CL-RFN89, the cell viability was measured with the Cell Counting Kit-8 using the WST-8 [2-(2-methoxy-4-nitrophenyl)-3-(4-nitrophenyl)-5-(2,4-disulfophenyl)-2*H*-tetrazolium, monosodium salt] assay. The number of viable cells was estimated and was shown as a ratio compared with an untreated control.

Ten wells were used for each cell and the average values were calculated. This experiment was repeated three times.

Mouse dorsal air sac assay

The mouse dorsal air sac assay was used to examine the effect of CL-RFN89 on the angiogenic response triggered by malignant tumor cells, according to a modification of the method described by Tanaka *et al.* (1989).

Both sides of a Millipore ring were covered with Millipore filters of 0.45-μm pore size and the Millipore chamber was filled with A431 tumor cells (1.5×10^6 cells) in 0.15 ml of PBS, with or without various concentrations of CL-RFN89. The chamber containing the A431 cells was implanted into an air sac formed previously in the dorsum of a 6-week-old female BALB/c mouse by injection of an appropriate volume of air. The control group implanted with the PBS-containing chamber was administered vehicle alone. On day 5, the implanted chambers were removed from the subcutaneous fascia of the treated mice. The angiogenic response was assessed in dissecting microscope photographs, by determining the number of newly formed blood vessels >3 mm in length within the area in direct contact with the chamber. The extent of angiogenesis was scored as 0, 1, 2, 3, 4 or 5, corresponding to the new formation of no, one, two, three, four or five or more blood vessels, respectively. The blood vessels newly formed in response to angiogenic factor(s) released from malignant tumor cells were morphologically distinct from the pre-existing vessels because of their zigzag characteristics, as described previously (Tanaka *et al.*, 1989).

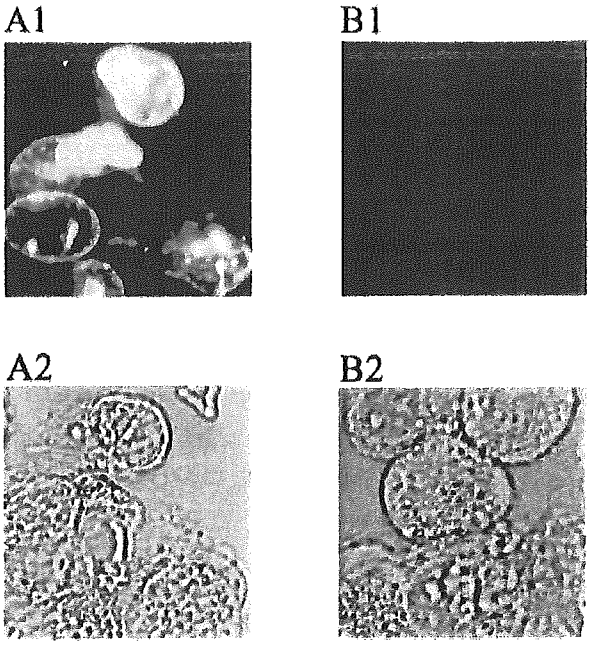

Fig. 1. FGF receptor-mediated binding of CL-RFN89 to HUVECs. The cells were incubated with fluorescein-labeled CL-RFN89 either alone (**A1**, **A2**) or complexed with an excess amount of bFGF (**B1**, **B2**) for 15 min (A1, A2 and B1, B2 are the same fields). The cells were thoroughly washed twice after incubation and a fluorescence microscope (A1, B1) and an optical microscope (A2, B2) were used to examine the cells.

Results

The binding reaction of CL-RFN89 with HUVECs

Our first series of experiments were designed to investigate whether the FGF–RNase fusion protein, CL-RFN89, reacts with the HUVECs specifically through the FGF receptor. We studied whether CL-RFN89 bound to the HUVECs in the presence of an excess amount of bFGF. When the cells were mixed with fluorescein-labeled CL-RFN89, the appearance of a green fluorescence on the cell surface was detected by fluorescence microscopy. On the other hand, no fluorescence was observed in the presence of an excess amount of bFGF (15 times the amount of CL-RFN89), even when substantial numbers of cells in the same fields were scanned under an optical microscope (Figure 1).

In vitro inhibition of angiogenesis by CL-RFN89

To examine whether CL-RFN89 inhibits the process of angiogenesis, we employed an *in vitro* model of angiogenesis in which HUVECs are induced to invade a three-dimensional collagen gel, where they form a network of capillary-like tubes. As shown Figure 2a, complex and branching capillary-tube like structures formed in a random fashion in the control group. In contrast, this dynamic process of *in vitro* angiogenesis was markedly inhibited in the presence of CL-RFN89.

Quantitative evaluation by measuring the length of the tubular structures was conducted and the ratio to the value in the control group was considered as an index of angiogenesis. CL-RFN89 inhibited angiogenesis in a dose-dependent manner and the length of the tubular structures formed was decreased to 43% of that in the control group in the presence of CL-RFN89 at a concentration of 2 μM (Figure 2b). However, these inhibitory effects were not observed and angiogenesis was in fact promoted when the cells were treated with an equimolar mixture (2 μM) of RNase1 and bFGF. These results demonstrated that CL-RFN89 suppressed the angiogenesis *in vitro*.

Cytotoxicity of CL-RFN89 against A431 cells and HUVECs

To confirm whether A431 cells and HUVECs can coexist with CL-RFN89 in the chamber, we assessed the cytotoxicity of this fusion protein by the use of the WST-8 before conducting the mouse dorsal air sac assay. CL-RFN89 inhibited the growth of HUVECs in a dose-dependent manner (Figure 3). On the other hand, the inhibition rate of the growth of A431 cells by CL-RFN89 was only 1.7% (Figure 3). In addition, no inhibition and proliferation were also observed when A431 cells were added with bFGF at a concentration from 0.1 to 10 μM (data not shown). This implied that CL-RFN89 did not exert any cytotoxicity against A431 cells and that these cells could therefore be applied for the following assay.

In vivo inhibition of tumor angiogenesis by CL-RFN89

Implantation of the chambers containing only PBS (negative control) was associated with minimal angiogenesis (Figure 4). The mean angiogenesis index was only 0.5 ± 1.22 ($N = 6$) (Figure 5), indicating that the experimental manipulation and subsequent healing process did not induce any significant angiogenic response. On the other hand, A431 cells separated by a semipermeable filter (positive control) triggered the neovascularization process, with an angiogenesis index of 4.4 ± 0.55 ($N = 5$). CL-RFN89 significantly suppressed the A431 cell-induced angiogenesis when the concentration of the chamber was kept at 1 and 2 μM. The mean angiogenesis

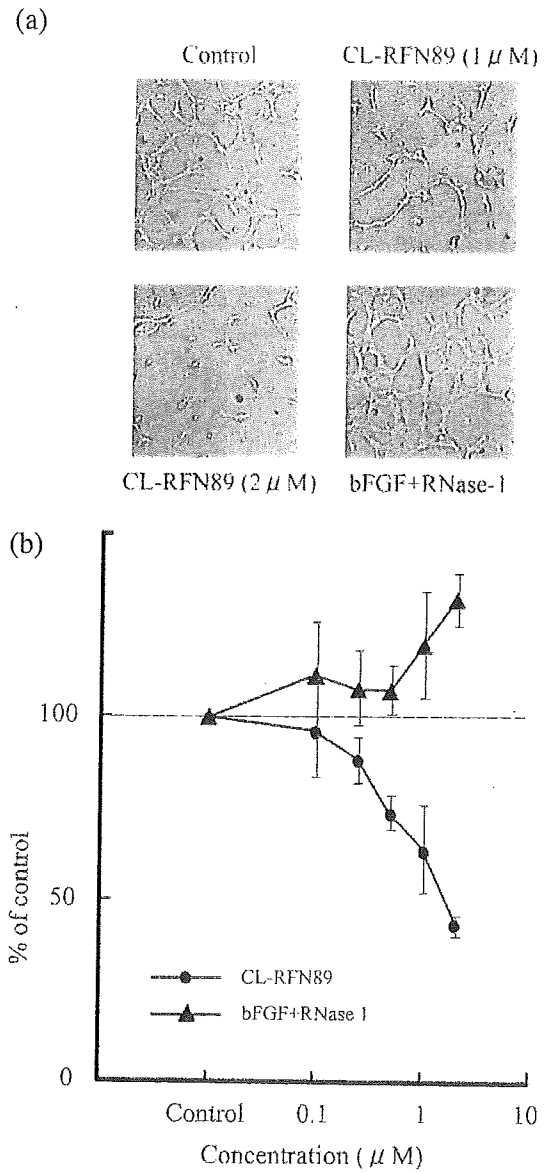

Fig. 2. Inhibition of capillary network formation by CL-RFN89 during 3D culture. (a) HUVECs were incubated in 3D culture for 4 h and treated with various concentrations of CL-RFN89. After incubation for 48 h, fields of tube-like structures were observed at random by an optical microscope (×40). Tube formation in the control HUVECs in 3D culture, HUVECs treated with CL-RFN89 (1 and 2 μM) and HUVECs treated with bFGF (2 μM) and RNase1 (2 μM) are shown. (b) Quantitative evaluation of the length of the tubular structure was performed by computer image analysis. The ratio of the group treated with CL-RFN89 (circles) and of the group treated with bFGF and RNase1 (triangles) to that in the control group was taken as the index of angiogenesis.

index was 0.8 ± 1.30 (N = 5) for both concentrations. As a control, the assay was used with RNase1 alone, bFGF alone and the buffer of same constituents with CL-RFN89, none of which proved to inhibit the angiogenesis (data not shown).

Discussion

Many immunotoxins, defined as proteins containing an antibody (or a ligand) and a toxin, have been developed to make

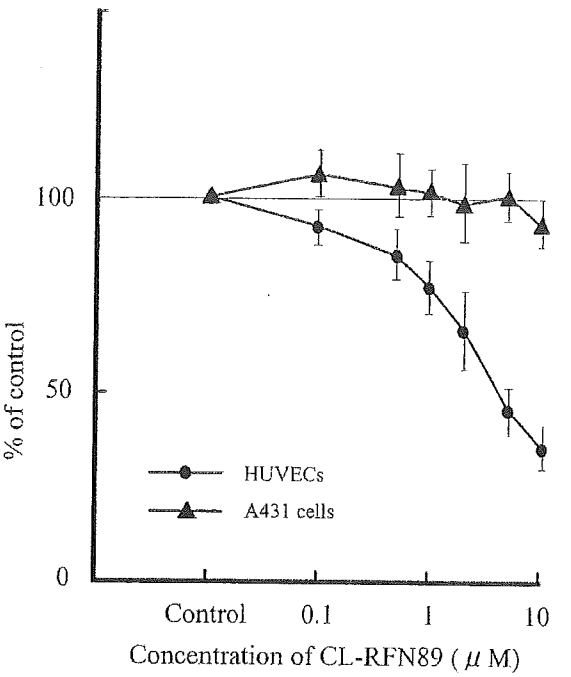

Fig. 3. Growth-inhibitory effects of CL-RFN89 on HUVECs and A431 cells. HUVECs (circles) and A431 cells (triangles) (10^4 cells/well) were cultured for 48 h with CL-RFN89. The growth of the cells in each well was monitored with Cell Counting Kit-8 and the absorbances were measured. The percentage growth relative to that of the cells treated with medium alone was calculated and plotted.

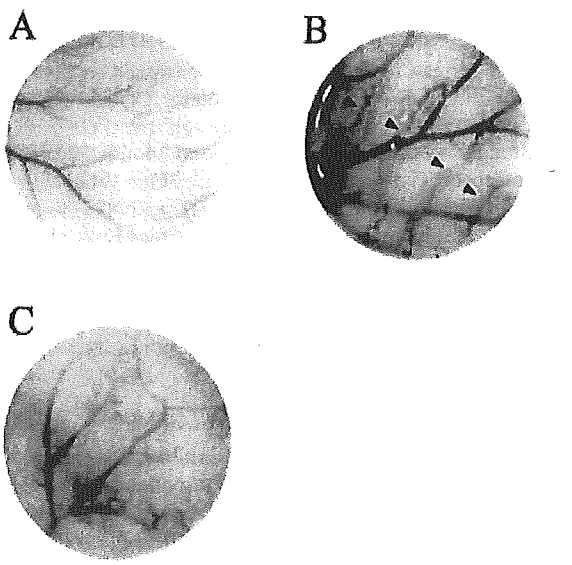

Fig. 4. Morphological study of the effect of CL-RFN89 on A431 cell-induced angiogenesis. The effectiveness of CL-RFN89 in causing suppression of tumor-induced angiogenesis was examined by the subcutaneous dorsal air sac technique. Groups A (**A**) and B (**B**) received implantation of chambers containing PBS and A431 tumor cells, respectively, and both were treated with the vehicle. Group C (**C**) received implantation of a chamber containing A431 tumor cells and CL-RFN89 (2 μM). On day 5 after implantation of the chamber, angiogenesis within the subcutaneous fascia was observed. Note that in (B), the chamber containing the A431 tumor cells induced the formation of blood vessels in a zigzag manner, characteristic of newly formed vasculature (arrowheads); this formation of new blood vessels was suppressed by treatment with CL-RFN89, as seen in (C).

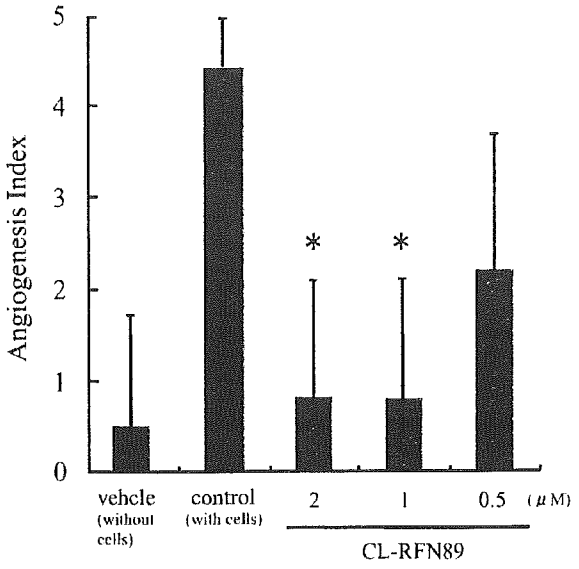

Fig. 5. Inhibitory effect of CL-RFN89 on the angiogenic response by A431 cells. Five days after the implantation of a chamber containing PBS or A431 tumor cells the effect of various concentrations of CL-RFN89 with A431 tumor cells on angiogenesis was assessed ($N = 5$). *$p < 0.001$ versus controls by Student's *t*-test.

use of tumor surface receptors and molecules and to obtain a differential effect between tumor cells and normal cells (Lappi *et al.*, 1990; Pastan *et al.*, 1998). Clinical applications are still limited, however, owing to the inherent toxicities of these substances to normal cells, in addition to their immunogenicity. The side effects therefore serve as dose-limiting factors for clinical application and efforts, focusing on mutations, deletions or other genetic manipulations on the toxin molecules to reduce their high toxicity are limited by the fact that the toxin's potency is also simultaneously reduced (Byers *et al.*, 1991; Vitetta *et al.*, 1993; Baluna *et al.*, 1997).

In an attempt to make it safer for clinical use, we and others have introduced the use of mammalian enzymes such as ribonucleases (RNases) instead of bacterial toxins (Rybak *et al.*, 1991; Jinno *et al.*, 1996; Psarras *et al.*, 1998). RNases constitute a large superfamily of proteins crossing over many species. Neither human RNases nor bovine pancreatic RNase A are themselves cytotoxic. However, when injected into *Xenopus* oocytes, they abolished protein synthesis at concentrations comparable to that of the toxin ricin by direct degradation of the cellular RNA (Rybak *et al.*, 1991; Saxena *et al.*, 1991).

Mammalian RNases are non-toxic to cultured cells and can be substituted for plant or bacterial toxins as an immunotoxin (Rybak *et al.*, 1995). However, it must enter the cell and reach the cytosol, where RNA degradation would ultimately lead to a cell death (Kim *et al.*, 1995; Wu *et al.*, 1995). In the cytosol, RNase encounters the ribonuclease inhibitor protein (RI). RI constitutes >0.01% of the total protein in the cytosol (Bretscher *et al.*, 2000) and it inactivates RNase by forming a tight complex that prevents RNA substrates from entering the active sites of the enzyme (Kobe and Deisenhofer, 1996). With the exception of bovine seminal RNase, which has been reported to be resistant to RI independently (Murthy *et al.*, 1996), it is important for RNase to possess the ability to evade RI in order to exert the desired cytotoxicity and several studies have been performed in this connection. It was shown that truncation of seven amino acid residues in the N-terminal sequence of RNase1 resulted in a more pronounced reduction in the affinity to human placental RI; however, it also significantly reduced the activity of the enzyme. A version of this 1–7 des RNase has 466-fold lower affinity to placental RI, while its ribonucleolytic activity is 8.6 times lower than that of RNase1 (Futami *et al.*, 1995) and it has no ability of cellular targeting. To maintain the activity of the enzyme, simultaneously reducing the affinity to RI and to achieve cellular targeting, bFGF was inserted genetically into Gly89 of RNase1 to prevent its stereostructural binding to RI. CL-RFN89 retained their activity at >85% even in the presence of 200-fold molar excess amount of RI and showed cell type-specific growth inhibition against malignant cells bearing FGF receptors (Tada *et al.*, 2004).

Our results for a binding assay using fluorescein-labeled CL-RFN89 showed that this protein could adhere to the cell surface of HUVECs. In the presence of an excess amount of unlabeled bFGF, however, no adhesion or uptake of CL-RFN89 to HUVECs occurred. This means that the excess bFGF occupies the FGF receptors and competitively prevent CL-RFN89 from binding to the cells, which suggests that the binding of the protein to HUVECs is FGF receptor dependent. This selective inhibition of CL-RFN89 for the HUVECs was also demonstrated in an *in vitro* cytotoxicity assay. CL-RFN89 inhibited the cellular growth of HUVECs, which express the FGF receptor (Chen *et al.*, 2001), in a dose-dependent manner. On the other hand, the growth of A431 human epidermal carcinoma cells remained intact despite the presence of CL-RFN89 at concentrations of up to 10 μM. Although it was previously reported that bFGF accelerated the growth of A431 cells *in vitro* (Sugimoto and Nishino, 1996), our result can be explained by a report showing that A431 cells express barely detectable levels of FGF receptor, by the analysis of [^{125}I]bFGF binding to A431 cells (Muggeridge *et al.*, 1992) and by a report showing that 16-mer oligopeptide, with conformation similar to the putative receptor-binding domain of bFGF had no ability to bind to A431 cells (Kono *et al.*, 2003). Furthermore, proliferation of A431 cells was not accelerated by bFGF at concentrations from 0.1 to 10 μM (data not shown).

In this study, CL-RFN89 was shown to exhibit antiangiogenic activity both *in vitro* and *in vivo*. Cytotoxicity assay showed that CL-RFN89 at a concentration of 10 μM caused 46% inhibition of the growth of HUVECs. It was thought that CL-RFN89 inhibited the proliferative phase of the cells. In the presence of CL-RFN89 at a concentration of 2 μM in the 3D culture system, the length of the tubular structures formed in the culture was decreased to 43% of that in the control group. The later stages of angiogenesis involve morphological alterations and functional maturation of endothelial cells, which result in lumen formation (Risau, 1997). These processes are controlled by the interaction of growth factors and extracellular matrix components (Folkman and Klagsbrun, 1987; Madri and Marx, 1992). By using the 3D culture system as an experimental model, we examined whether CL-RFN89 inhibited the remodeling phase of angiogenesis, corresponding to the late phase (Madri and Marx, 1992; Marx *et al.*, 1994; Prols *et al.*, 1998). It was revealed that a specific expression pattern of transmembrane receptors, including the FGF receptor and induction of a new set of differentiation-specific genes, occurred during the course of angiogenesis (Marx *et al.*, 1994; Sankar *et al.*, 1996).

CL-RFN89 had the ability to inhibit the process of angiogenesis at this point *in vitro*. In addition, CL-RFN89 was also shown to inhibit angiogenesis by the mouse dorsal air sac assay. Neovascularization of the mouse subcutaneous tissues, which was triggered by A431 cells, was effectively inhibited by the administration of CL-RFN89. This result was not caused by the growth suppression of A431 cells in the membrane chamber, because the growth of these cells was shown to be unaffected by CL-RFN89 in the cytotoxicity assay. It was assumed that CL-RFN89 infiltrated the surrounding tissues through the membrane filter and inhibited vascularization by the cells, bearing FGF receptors, such as the endothelial cells, the smooth muscle cells and the others responsible for the neovascularization. These results show that CL-RFN89 is a potent inhibitor of angiogenesis.

Recent studies have examined the role of FGF receptors in tumor growth and several tumor cell lines that express FGF receptors on their cell surface. Amplification of the FGFR1 and FGFR2 genes in breast tumor tissues from over 350 patients was examined and it was found to occur in ~10% of the patients (Adnane *et al.*, 1991). Screening of breast tumor cell lines or tissues for FGFR4 revealed overexpression of the FGFR4 mRNA (Lehtola *et al.*, 1992; Ron *et al.*, 1993; Penault-Llorca *et al.*, 1995), suggesting that FGFR4 may have a role in the development of breast cancer in humans. FGF has also been implicated as an autocrine growth factor for melanomas (Halaban *et al.*, 1987), gliomas, meningiomas (Ueba *et al.*, 1994) and pancreatic ductal adenocarcinomas (Kornmann *et al.*, 1998). This expression of FGFR may provide a mechanism for targeting tumor cells. It was observed that CL-RFN89 exerted efficient growth inhibition of mouse metastatic melanoma B16/BL6 cells *in vitro* (Tada *et al.*, 2004). An *in vivo* study using tumor cell lines expressing FGFR is now under way in order to demonstrate the therapeutic potential of CL-RFN89. It is expected that CL-RFN89 would exhibit anti-tumor activity both by a direct effect (inhibition of tumor cell growth) and by an indirect effect (inhibition of tumor angiogenesis). It may be possible to devise a new strategy by utilizing the synergism between the direct and indirect anti-tumor activities of this compound.

In summary, our results provided evidence that the bFGF–RNase fusion protein could be efficiently targeted via the FGF receptors in HUVECs and that this protein inhibited proliferation and tube formation of the cells *in vitro*. In addition, this protein also effectively inhibited tumor angiogenesis *in vivo*. These experiments have demonstrated that tumor angiogenesis can be targeted by CL-RFN89 via FGF receptors and that this protein holds promises as an antiangiogenic agent that exerts specificity for the cells bearing the FGF receptors.

Acknowledgements

The authors thank Mrs Yuki Nakamura for her technical support and helpful discussions. This research was supported by the Ministry of Education, Culture, Sports, Science and Technology Grant-in-Aid for Scientific Research (B) and Grant-in-Aid for the 21st Century Center of Excellence (COE) Program entitled 'Establishment of individualized cancer therapy based on comprehensive development of minimally invasive and innovative therapeutic methods (Keio University)'.

References

Adnane,J., Gaudray,P., Dionne,C.A., Crumley,G., Jaye,M., Schlessinger,J., Jeanteur,P., Birnbaum,D. and Theillet,C. (1991) *Oncogene*, **6**, 659–663.
Baluna,R. and Vitetta,E.S. (1997) *Immunopharmacology*, **37**, 117–132.
Blanckaert,V.D., Schelling,M.E., Elstad,C.A. and Meadows,G.G. (1993) *Cancer Res.*, **53**, 4075–4081.
Bretscher,L.E., Abel,R.L. and Raines,R.T. (2000) *J. Biol. Chem.*, **275**, 9893–9896.
Byers,V.S. and Baldwin,R.W. (1991) *Semin. Cell Biol.*, **2**, 59–70.
Chen,J.H., Wang,X.C., Kan,M. and Sato,J.D. (2001) *Cell Biol. Int.*, **25**, 257–260.
de Jong,J.S., van Diest,P.J., van der Valk,P. and Baak,J.P. (1998) *J. Pathol.*, **184**, 53–57.
Folkman,J. (1992) *Semin. Cancer Biol.*, **3**, 65–71.
Folkman,J. and Klagsbrun,M. (1987) *Science*, **235**, 442–447.
Folkman,J. and Shing,Y. (1992) *J. Biol. Chem.*, **267**, 10931–10934.
Futami,J., Seno,M., Kosaka,M., Tada,H., Seno,S. and Yamada,H. (1995) *Biochem. Biophys. Res. Commun.*, **216**, 406–413.
Futami,J., Seno,M., Ueda,M., Tada,H. and Yamada,H. (1999) *Protein Eng.*, **12**, 1013–1019.
Futami,J., Tsushima,Y., Tada,H., Seno,M. and Yamada,H. (2000a) *J. Biochem. (Tokyo)*, **127**, 435–441.
Futami,J., Tada,H., Seno,M., Ishikami,S. and Yamada,H. (2000b) *J. Biochem. (Tokyo)*, **128**, 245–250.
Giavazzi,R., Giuliani,R., Coltrini,D., Bani,M.R., Ferri,C., Sennino,B., Tosatti,M.P., Stoppacciaro,A. and Presta,M. (2001) *Cancer Res.*, **61**, 309–317.
Griffin,R.J., Williams,B.W., Wild,R., Cherrington,J.M., Park,H. and Song,C.W. (2002) *Cancer Res.*, **62**, 1702–1706.
Hagedorn,M., Zilberberg,L., Lozano,R.M., Cuevas,P., Canron,X., Redondo-Horcajo,M., Gimenez-Gallego,G. and Bikfalvi,A. (2001) *FASEB J.*, **15**, 550–552.
Halaban,R., Ghosh,S. and Baird,A. (1987) *In Vitro Cell Dev. Biol.*, **23**, 47–52.
Jinno,H., Ueda,M., Ozawa,S., Kikuchi,K., Ikeda,T., Enomoto,K. and Kitajima,M. (1996) *Cancer Chemother. Pharmacol.*, **38**, 303–308.
Karp,J.E. and Broder,S. (1995) *Nat. Med.*, **1**, 309–320.
Kim,J.S., Soucek,J., Matousek,J. and Raines,R.T. (1995) *J. Biol. Chem.*, **270**, 31097–31102.
Klint,P. and Claesson-Welsh,L. (1999) *Front. Biosci.*, **4**, D165–D177.
Kobe,B. and Deisenhofer,J. (1996) *J. Mol. Biol.*, **264**, 1028–1043.
Kono,K., Ueba,T., Takahashi,J.A., Murai,N., Hashimoto,N., Myoumoto,A., Itoh,N. and Fukumoto,M. (2003) *J. Neurooncol.*, **63**, 163–171.
Kornmann,M., Beger,H.G. and Korc,M. (1998) *Pancreas*, **17**, 169–175.
Lappi,D.A. and Baird,A. (1990) *Prog. Growth Factor Res.*, **2**, 223–236.
Lehtola,L., Partanen,J., Sistonen,L., Korhonen,J., Warri,A., Harkonen,P., Clarke,R. and Alitalo,K. (1992) *Int. J. Cancer*, **50**, 598–603.
Li,W.W. (2000) *Acad. Radiol.*, **7**, 800–811.
Madri,J.A. and Marx,M. (1992) *Kidney Int.*, **41**, 560–565.
Marx,M., Perlmutter,R.A. and Madri,J.A. (1994) *J. Clin. Invest.*, **93**, 131–139.
Muggeridge,M.I., Cohen,G.H. and Eisenberg,R.J. (1992) *J. Virol.*, **66**, 824–830.
Murthy,B.S., De Lorenzo,C., Piccoli,R., D'Alessio,G. and Sirdeshmukh,R. (1996) *Biochemistry*, **35**, 3880–3885.
O'Reilly,M.S., Holmgren,L., Chen,C. and Folkman,J. (1996) *Nat. Med.*, **2**, 689–692.
O'Reilly,M.S., Boehm,T., Shing,Y., Fukai,N., Vasios,G., Lane,W.S., Flynn,E., Birkhead,J.R., Olsen,B.R. and Folkman,J. (1997) *Cell*, **88**, 277–285.
Pastan,I.I. and Kreitman,R.J. (1998) *Adv. Drug Deliv. Rev.*, **31**, 53–88.
Penault-Llorca,F., Bertucci,F., Adelaide,J., Parc,P., Coulier,F., Jacquemier,J., Birnbaum,D. and deLapeyriere,O. (1995) *Int. J. Cancer*, **61**, 170–176.
Prols,F., Loser,B. and Marx,M. (1998) *Exp. Cell Res.*, **239**, 1–10.
Psarras,K., Ueda,M., Yamamura,T., Ozawa,S., Kitajima,M., Aiso,S., Komatsu,S. and Seno,M. (1998) *Protein Eng.*, **11**, 1285–1292.
Risau,W. (1997) *Nature*, **386**, 671–674.
Ron,D., Reich,R., Chedid,M., Lengel,C., Cohen,O.E., Chan,A.M., Neufeld,G., Miki,T. and Tronick,S.R. (1993) *J. Biol. Chem.*, **268**, 5388–5394.
Rybak,S.M., Saxena,S.K., Ackerman,E.J. and Youle,R.J. (1991) *J. Biol. Chem.*, **266**, 21202–21207.
Rybak,S., Newton,D. and Xue,Y. (1995) *Tumor Targeting*, **1**, 141–147.
Sankar,S., Mahooti-Brooks,N., Bensen,L., McCarthy,T.L., Centrella,M. and Madri,J.A. (1996) *J. Clin. Invest.*, **97**, 1436–1446.
Saxena,S.K., Rybak,S.M., Winkler,G., Meade,H.M., McGray,P., Youle,R.J. and Ackerman,E.J. (1991) *J. Biol. Chem.*, **266**, 21208–21214.
Seghezzi,G., Patel,S., Ren,C.J., Gualandris,A., Pintucci,G., Robbins,E.S., Shapiro,R.L., Galloway,A.C., Rifkin,D.B. and Mignatti,P. (1998) *J. Cell Biol.*, **141**, 1659–1673.
Sugimoto,H. and Nishino,H. (1996) *Hum. Cell*, **9**, 129–140.
Tada,H., Onizuka,M., Muraki,K., Masuzawa,W., Futami,J., Kosaka,M., Seno,M. and Yamada,H. (2004) *FEBS Lett.*, **568**, 39–43.